1985

The Effects of Magnetic Flux on Suspended Particles in Seawater

Mohammed A. Nehme
University of Central Florida

STARS Citation

Nehme, Mohammed A., "The Effects of Magnetic Flux on Suspended Particles in Seawater" (1985). *Retrospective Theses and Dissertations*. 4801.
https://stars.library.ucf.edu/rtd/4801

THE EFFECTS OF MAGNETIC FLUX ON SUSPENDED PARTICLES IN SEAWATER

BY

MOHAMMED A. NEHME
B.S., University of Florida, 1982

THESIS

Submitted in partial fulfillment of the requirements
for the degree of Master of Science in Engineering
in the Graduate Studies Program of the College of Engineering
University of Central Florida
Orlando, Florida

Fall Term
1985

ABSTRACT

A study was conducted to investigate the effect of magnetic devices on the precipitates in a condenser's tubes when seawater is used as cooling water. This test was necessary to evaluate these devices as possible replacements for conventional methods of water treatment.

In the test program, a small condenser was operated with conditions similar to utility condensers. This condenser was modified to include twelve tubes. The inlet water box was divided to provide for two parallel magnetic water treatment streams, and one control untreated water stream for comparison purposes. With and without the use of a magnetic device, the chemical analysis and the thickness of the deposits showed no significant difference. The only difference that was observed in these deposits was their crystallogical structure.

When the magnetic device was in place, deposits were flaky (powder-like), chipped, and showed no strong adhesion to the inner surface of the condenser's tubes. Without the use of a magnetic device, deposits were flocculated, hard, and crusty.

This thesis proposes a theory which may help explain the differences in the deposits. The theory will include homogeneous nucleation to explain the physical changes of the deposits. The discussion will also postulate how well the magnetic energy improved the homogeneous nucleation process. A method of analysis is proposed which demonstrates how the critical radius of a nucleus is affected by a magnetic field.

ACKNOWLEDGEMENTS

The author wishes to acknowledge the financial support received from the University of Central Florida for the completion of his graduate study.

Mr. Nehme wishes to thank the faculty who served on his Committee. He would like to acknowledge Dr. E. R. Hosler, Mr. R. L. Henry, Mr. A. Minardi and Dr. P. J. Bishop. Special appreciation is extended to Dr. E. R. Hosler and Mr. R. L. Henry for their continuing encouragement, support, advice and their valuable suggestions during this study.

The author also wishes to acknowledge the help and technical advice of the R&D Shop of the College of Engineering, especially to Mr. Cecil W. Poston and Mr. David Ackerson. Also, a special thanks is addressed to the Department of New Technology of the Florida Power Corporation, especially to Mr. Michael Rib who helped the author in completing the experimental part of this project.

The author is also indebted to Mrs. Linda Stewart for her perfect typing job.

TABLE OF CONTENTS

LIST OF TABLES

LIST OF FIGURES

LIST OF SYMBOLS

a	Acceleration
A	Constant for a particular process
C_1, C_2	Number of solute atoms
D	Diffusion coefficient
D_o	Diffusion coefficient independent of temperature
E	Total energy of an atom
E_m	Activation energy for vacancy motion
E_v	Activation energy for vacancy formation
ΔE	Internal energy change
ΔE_v	Internal energy change per unit volume
F	Coulomb force
f	Resultant force
γ	Surface energy change
ΔG	Free energy change
ΔG^*	Critical total free energy change
ΔG_T	Total free energy change
ΔG_v	Free energy change per unit volume
ΔG_{vm}	Free energy change per unit volume in the presence of a magnetic energy
ΔG_m	Free energy change in the presence of magnetic energy
ΔG^*_m	Critical free energy in the presence of magnetic energy

J	Net flux
K	Boltzmann's constant
K_E	Kinetic energy
M	Mass
Δ_M	The change in magnetic energy
N	Number of lattice sites
N_v	Number of vacancies
P	Probability
P_E	Potential energy
Q_1, Q_2	Charge of particles
R	Rate of reaction
r'	Initial separation distance
r''	Final separation distance
r	Radius of a sphere
r^*	Critical radius of a sphere
r^*_m	Critical radius in the presence of magnetic energy
T	Absolute temperature
ΔT	Temperature difference
T_e	Temperature value under a specific condition
u	Frequency
v	Velocity

INTRODUCTION

It is convenient for utility plants, built in coastal areas, to utilize seawater as a cooling agent for the condenser. The consequences of using saltwater are the rapid growth of bacteria and the build-up of salts and minerals. These minerals form hard scales which can cause pitting and corrosion that eventually damage the condenser's tubes. These problems are solved by shutting down the condenser periodically, and cleaning its tubes with chemical products. In addition, the use of chemical treatment is expensive, and it has caused water pollution. Therefore, alternative methods to clean the condenser's tubes are desirable. One alternative is magnetic conditioning. Several manufacturers of magnetic water treatment devices claim that passing the water through a magnetic field affects the water in a manner similar to chemical water softening, and it would eliminate the need for frequent shutdown of the condenser.

Many research papers pertaining to this subject have been published in the Soviet Union, with only a few published in the United States. In these papers, many different ideas are discussed about the magnetic treatment of fresh water. Some investigators stated that the magnetic treatment of water does not affect water in a manner similar to chemical water softeners. Others emphasized that the magnetic treatment conditioned the water. However, to this date there is no documented experience in the use of magnetic devices for the conditioning of seawater when used as cooling water for condenser.

The purpose of this research project, recently completed by the University of Central Florida and sponsored by Florida Power Corporation, was to conduct a controlled experiment to evaluate the effectiveness of magnetic water treatment of seawater for condenser application.

Primarily this test program consisted of the use of a small condenser and a vacuum boiler. An existing condenser was modified to include three sections of four tubes each. The magnetically treated seawater was introduced to two of the sections, while the third was used as the control and left untreated. The flow rate of cooling water through each section was maintained at 55 gallon per minute (GPM). This condenser was designed to operate under conditions prototypical of power plant's condensers. The condenser, the vacuum boiler, and their accessories (PVC pipes, instruments, etc...) were installed at Florida Power's Bayboro facility in St. Petersburg, Florida. This prototype condenser was in operation for nine months. During the testing, the condenser was shut down periodically to remove the tubes for deposit inspections. Each time the tubes were removed, the accumulated deposits were inspected for degree of adherence, and to measure the average thickness of the deposits in each tube. It was observed that deposits, accumulated in tubes which received treated water, were less adherent to tube walls than deposits built-up in tubes that received untreated water. The difference in the average thickness of deposits between each tube was not significant. During the period of operation, three measurements of deposit thickness, two chemical analyses, and several inspections for the deposits were made. This was necessary to assure consistency in the results stated above.

The proposed operation includes homogeneous nucleation. In this test program, the chemical analysis indicated that the elements and the compounds of deposit, found in all tubes were the same. In addition, these deposits had an approximate film thickness that was uniform around the inner surface of all tubes. Therefore, from the above observation, an affirmation can be stated that the deposits were homogeneous in all the tubes. However, it was observed that the physical characteristics of deposits, scraped from tubes that received untreated water, were different than the deposits scraped from tubes that received treated water. This indication reveals that the magnetic energy had affected the homogeneity of the deposits scraped from tubes that received treated water.

Homogeneous nucleation is a process explaining the formation and growth of a crystal. The physical structure of a crystal, at the atomic level, is composed of molecules. To form a molecule, a group of atoms are attracted to each other by a force. This force is categorized into two groups: a strong interatomic force and a small interatomic force. These facts also hold true for the molecules themselves. Molecules can be modeled as hexagonal close pack

(HCP) and/or face centered cubic (FCC) types. These two types generally describe the physical structure of a structure. Since the structure of crystals is not ideal, they contain structural imperfections at the atomic level. The study of structural imperfection in crystals has lead scientists to develop many theories to understand the behavior of matter. The intensive research in this area includes the application of the first and the second laws of thermodynamics. These laws were used to calculate the number of vacancies in a crystal. They were manipulated into equations that, mathematically, describe the atom's motion. Since the motion of atoms occur randomly, the diffusion process decribed by Fick's law was developed to enhance the further understanding of this motion. It is indicated that self-diffusion will occur by a vacancy mechanism, and by an interstitial mechanism.

Introduction to the physical structure of a crystal, and to the dynamic motion processes associated with this structure have been presented. The equations describing these processes will be applied in another process, the homogeneous nucleation process. However, the objective is to achieve a full understanding about the formation, the size, the rate and the growth of a crystal. These subjects are discussed in detail in Chapter 3. They fall under the following headings: the Kinetics of Phase Change, Homogeneous Nucleation, Rate of Nucleation, and Growth of a Nucleus. Using the contents of these topics, the main goal in this thesis is to accomplish a plausible explanation as to how magnetic energy will affect the homogeneous nucleation process, and the rate of growth of a nucleus.

REVIEW OF THE EXPERIMENT

The primary objective of the experiment was to test and evaluate the effectiveness of the magnetic water treatment of seawater. The test equipment consisted of a condenser, vacuum boiler, two centrifugal pumps, and connecting PVC pipes. Three different types of magnetic devices were tested during the nine and one-half months of operation.

The testing was conducted at Florida Power's Bayboro plant. During the test period the system was shut down periodically to measure deposit thicknesses and to analyze the contents of these deposits. Based upon these results the magnetic devices were evaluated for effectiveness.

Condenser

Originally, the condenser used in this experiment, Figure 1, contained ten 1-inch diameter tubes, each of which were ten feet in length. The end plate of the inlet water box was specially made from stainless steel material to hold four ultrasonic transducers, and had one opening for the entry of water. These were made available followng a previous test program.

For the purpose of this experiment, some modifications of the condenser were required. First, the end plate of the inlet water box was cut and replaced by another plain plate which was fabricated

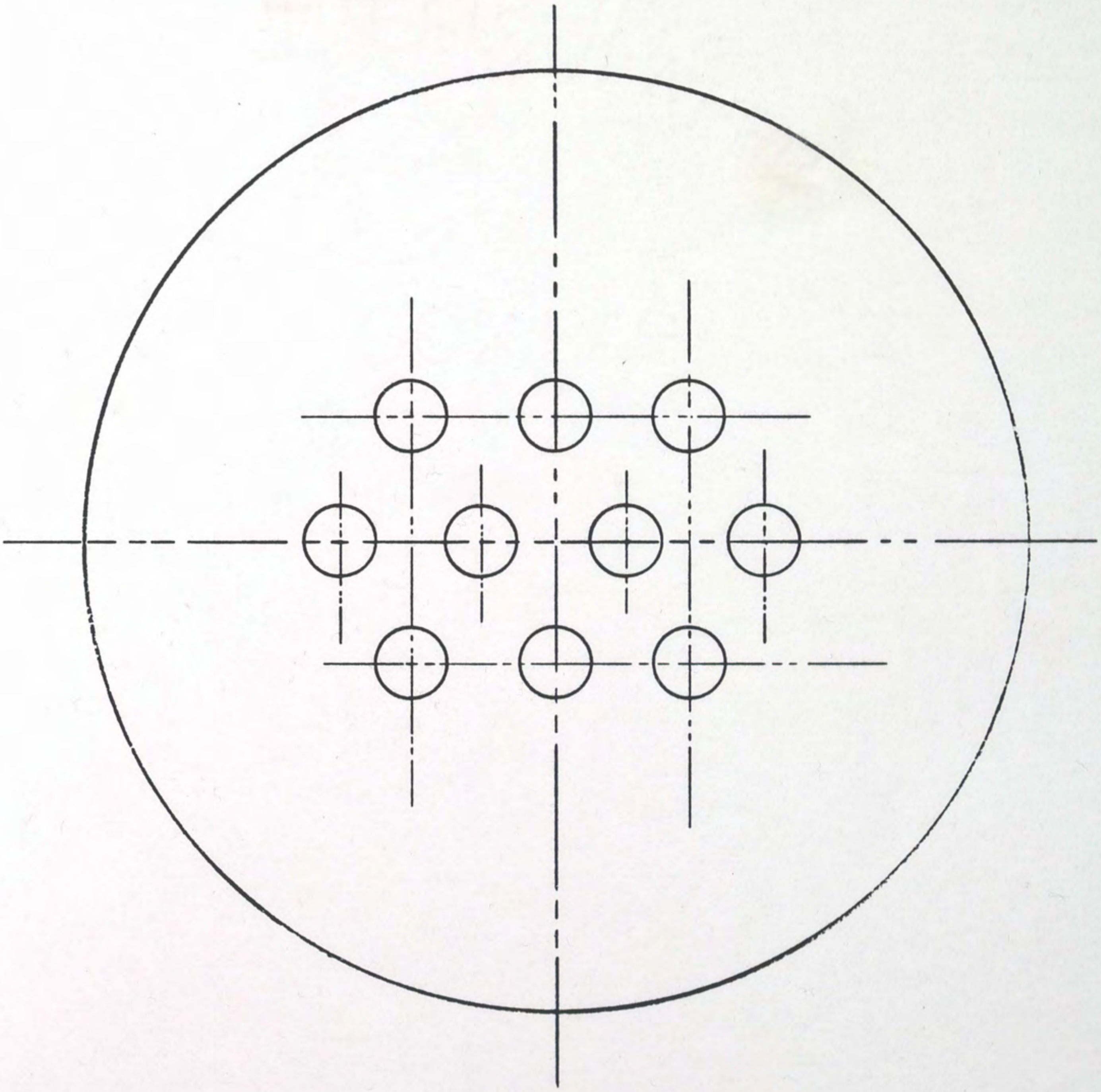

FIGURE 1. INLET TUBE SHEET BEFORE MODIFICATION.
NOTE: Each tube is ten-foot long.

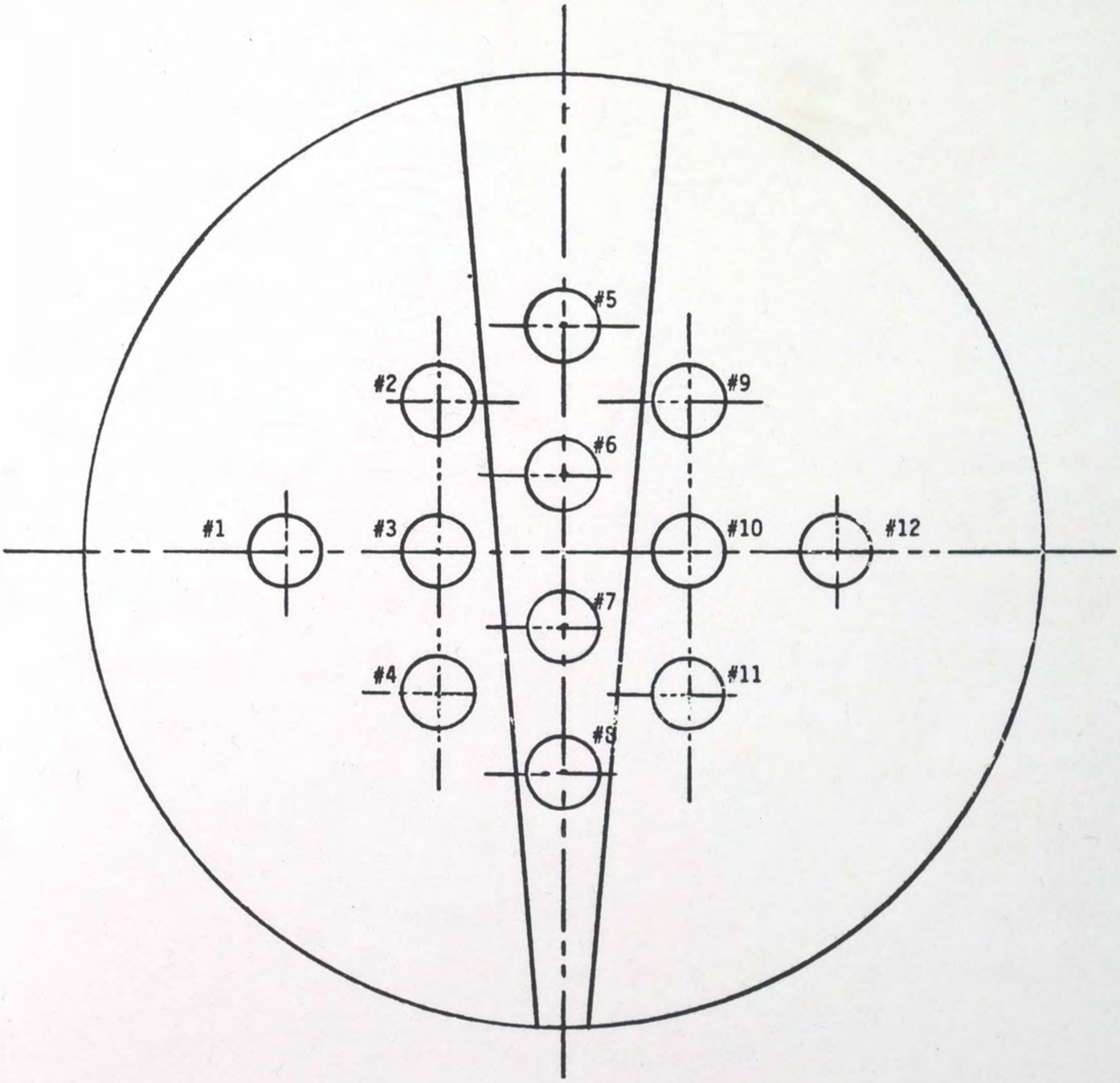

FIGURE 2. INLET TUBE SHEET AS MODIFIED.

NOTE: Tubes #1, 2, 3, and 4 were exposed to to linear kinetic cell treatment unit. Tubes #5, 6, 7 and 8 were exposed to untreated water. Tubes #9, 10, 11 and 12 were exposed to turbomag treatment unit from 12/14/83 to 5/1/84 and to hydrodynamics treatment unit from 5/1/84 to 3/17/84.

at the University of Central Florida R&D Shop. Second, two additional condenser tubes, Figure 2, were added (making a total of 12 tubes). Next the inlet water box was subdivided into three sections, where each had one opening for the entry of water, and to provide for two parallel magnetic water treatment streams and one control untreated water stream for comparison purposes. Three holes were drilled in the end plate of the exit water box to measure the exit seawater temperature. The exit water box had one opening for the return of water to the bay.

On the side shell of the consider, one 2.5-inch diameter steam supply pipe and one one-inch diameter condensate return pipe were provided. There was one valve in each pipe to control and balance the quantity of the incoming steam with the return condensate to the boiler. An appropriate frame was built for this condenser to support it.

Boiler

Basically, the boiler is a circular tank with 16 electric heaters. The top and bottom round plates are 36 inches in diameter and the height of the boiler is 30 inches. A fill plug and steam exhaust line to the condenser were attached to the top of the boiler. On the side of the boiler, a one-inch opening received the return condensate from the condenser's hot well. Finally, a visual sight glass was provided to observe the water level inside the boiler. In this test program, no major modifications were made on this boiler.

Apparatus Assembly

Other equipment used in this test program consisted of two centrifugal pumps, a calibrated flow meter, three magnetic water treatment units, interconnecting PVC piping, orifice plates, and a temperature indicator. During the test period, only two magnetic devices were tested at a time.

The two centrifugal pumps of 4.2 and 2.8 HP, Figure 3, were used in series to provide cooling water to the condenser. This cooling water was Tampa Bay water taken from the old steam plant's intake canal. The pumps then discharged into a 3-inch line which was divided into three 1.5-inch lines. In two of these three lines the magnetic treatment units were installed, while the third line was connected directly to the condenser inlet. Each line contained a flow control valve to regulate the flow, and a 0.5-inch diameter orifice plate, in conjunction with a mercury manometer. The three lines then supplied water to their individual sections in the inlet water box of the condenser.

The condenser exit water box was connected to a 3-inch discharge line through which the effluent was returned. The shell and water boxes of the condenser were made from carbon steel, the tube sheets were muntz metal, and the tubes used in this test were 90:10 copper nickel.

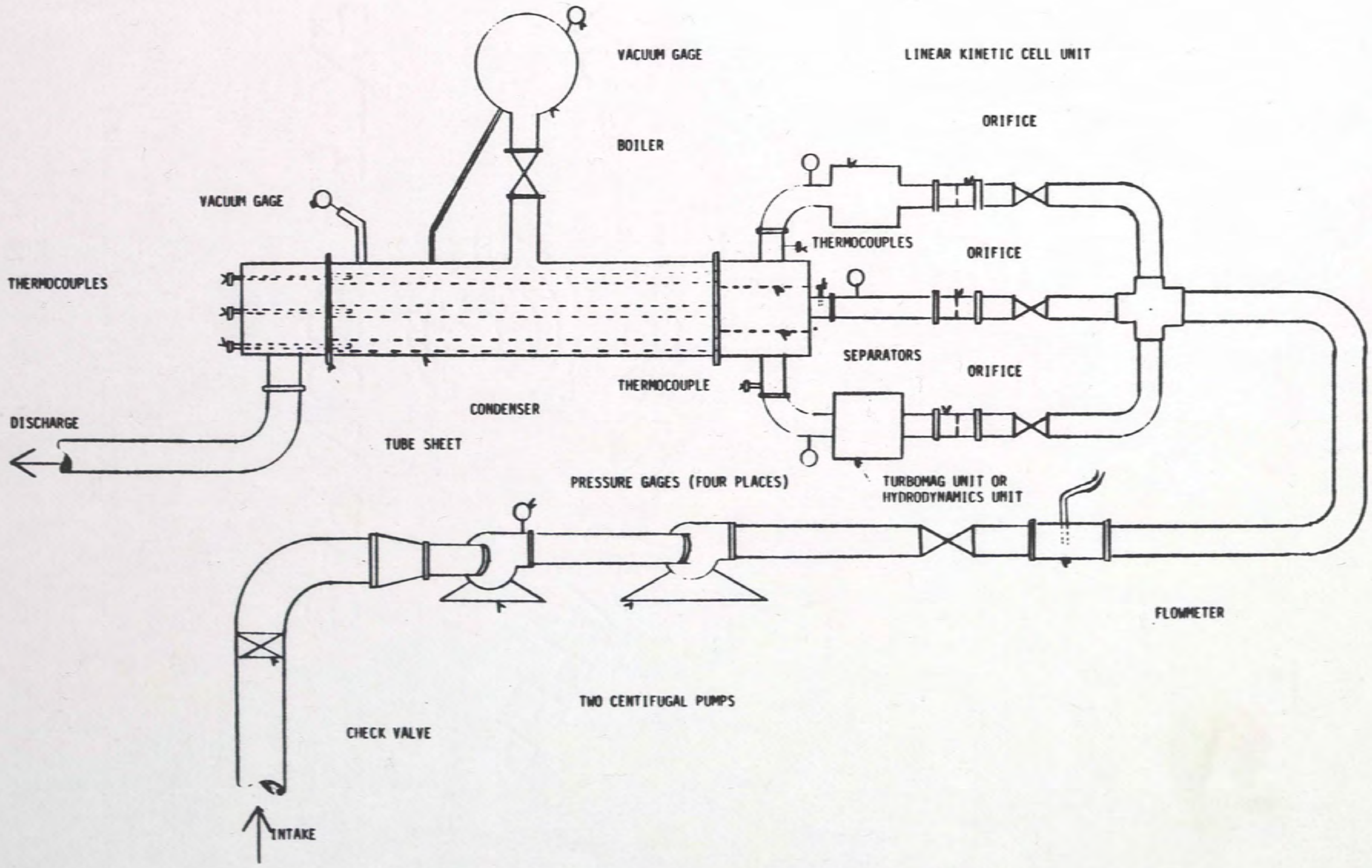

FIGURE 3. SCHEMATIC OF TEST FACILITY.

Instrumentation

To monitor the proper operation of the system, different instruments were used. Mercury manometers were connected across each orifice plate in the three supply lines that provided cooling water to the inlet water box. It was determined that the flow rate in each supply line should be maintained at approximately 55 gallons per minute to provide a velocity of 7 ft/sec in the condenser tubes. Therefore, the necessary pressure drop across each orifice was calculated at 3-inches of mercury. Just upstream of the inlet water box, Bourdon tube pressure gages were connected to each of the 1.5-inch supply lines, and also to the discharge line located downstream of the exit water box. The gages were necessary to monitor the pressure drop across the condenser, and they were used to check for leaks and/or blockages in the supply lines. Bourdon tube vacuum gages were connected to the top plate of the boiler and to the highest point of the condenser, to ensure that the steam exhaust pressures were near that of the typical low pressure turbine exhausts in a power plant. Seven stainless steel sheathed chromel-alumel thermocouples were used in this test. One was inserted into each inlet supply line, just upstream of the inlet water box. Three were inserted into the exit water box of the condenser. These thermocouples were used to monitor the differential temperature across the condenser. The last thermocouple was inserted into the boiler, and was connected to a control temperature box. The control temperature box was connected to the heaters to ensure that heat was added properly whenever the temperature of the water in the boiler went below 120F to maintain vacuum conditions similar to turbine exhaust.

Operational Procedure

An operational procedure of the system described in Figure 3 was to create a vacuum. This was accomplished by means of a vacuum pump on the condenser and boiler system to evacuate most of the air. Several heaters were turned on and the boiler was brought to boiling at the vacuum pressure indicated by the gage. Then the boiler was allowed to boil until the pressure in the condenser and boiler system reached 5 PSI above atmospheric pressure. Next, the pressure relief valve which was installed at the highest point on the condenser, just above the condenser's vacuum gage, was opened until the pressure in the boiler and condenser reached atmospheric pressure. This was done to remove any trapped air from the system. The relief valve was then closed and the two centrifugal pumps were turned on to supply cooling water to the condenser. The sudden collapsing of the steam drew a vacuum on the boiler and condenser system. The heaters were turned on, and the boiler temperature controller was then adjusted to maintain the boiler temperature at 120F.

Once the above steps were completed, the flow rate of the cooling water was adjusted to 55 gallons per minute in each supply line. Then, the magnetic treatment units were turned on.

Temperatures and pressure across the condenser were recorded periodically for several hours, until steady state operation was achieved.

Routine Operation

During the testing program, the system operation was monitored on a weekly basis. In each inspection period, temperatures and pressures were recorded and mechanical adjustments were made as necessary including adjustment of the cooling water flow back to its desired value, and cleaning the pump's suction line. In the early stages of testing, it was difficult to keep the cooling water flow at 55 gallons per minute in each supply line. The cause of the difficulty was resolved after inspecting the inlet suction line of the 4.2 HP pump, where debris and other suspended materials were the cause of the reduction in the cooling water flow rate. To correct this problem, a large "chicken wire screen" was placed over the cooling water inlet suction line.

After the above problem was corrected, the condenser was inspected at monthly intervals. During these inspections, the condenser was shut down and the inlet and outlet water boxes were removed to permit visual inspection of the deposits on the water boxes' surface and tube surfaces.

Sampling Methods

Originally, it was planned to inspect the condenser's tubes visually every two months. This inspection involved the removal of the inlet and exit water boxes, and careful observation of the build-up of deposits inside the tubes. After the first inspection was made, it was decided to remove Tube #1, which received treated water from the linear kinetic cell, Tube #6, which received untreated water, and tubes #9 and #12, which received treated water from the turbomag unit.

During the first tube removal, a tube became lodged inside the condenser, which made it necessary to remove both tube sheets and retube the entire condenser. Since this tube removal operation was very time-consuming, both the University of Central Florida (UCF) and the Florida Power Corporation decided to utilize an experienced crew provided by Florida Power. The crew performed subsequent tube removals on June 30 and August 7, 1984.

Each time the tubes were removed from the condenser, the deposits near the exits of the tubes were examined for their physical characteristics. The purpose of these physical tests was to check the adherence of the deposits in the tubes. These tests were done by wiping the deposit from the tubes' surface, with a finger, and noting the degree of adherence in the tube. The results of these tests showed no significance differences in any of the tubes. Immediately following each physical observation, the tubes were numbered, and tube ends covered to keep the deposits from drying out or flaking off tube surfaces. The tubes were then brought to the Material Science Laboratory at UCF for detailed examination.

In examining the deposits found on the surfaces of the tubes, three inspections were made. The first was to determine the physical characteristics and the degree of deposit adherence. The second was to determine the deposit thickness, and the third test was to determine the chemical composition of the deposits.

The first and second tests of the deposits, the results were obtained at UCF due to the availability of appropriate equipment. However, to obtain results concerning the third test, deposit samples were sent to the Material Science and Engineering Department at the University of Florida for chemical analysis.

To perform the second inspection, the examiner physically compared two five-inch pieces of tube, one treated and the other untreated. By tapping both pieces of tube on a solid surface, it was noted that the treated tube's deposit was more easily shaken off than those of the untreated tube.

To accomplish the second, the examiner selected and filled one inch axial segments of tube with metallurgical casting resin, for the stabilization of the materials. The specimen tubes were placed in a vacuum and allowed to dry for two days until the resin became solid. The specimens were then polished on a revolving wheel. This allowed easy identification of deposit thickness. Then the deposit thickness was measured at various circumference points, for each specimen, by using a measuring metallurgical microscope. Chemical analysis, as mentioned before, was performed at the University of Florida where both elemental and compound analyses were performed using an energy dispersive spectrometry.

RESULTS

Operating Cycle

On December 15, 1983, the system was initially placed into operation. During the first month of operation problems were encountered in maintaining the cooling water flow at 55 gallons per minute in each supply line, and in operating the boiler properly. During the first inspection on January 16, 1984, there was difficulty in removing individual tubes, which made it necessary to remove both tube sheets, retube the whole condenser, and restart the experiment. These problems were corrected as explained in the previous paragrahs.

During the first inspection, on January 16, 1984, measurement of the deposit thicknesses showed that the deposit film was very thin, and that there was no significant difference in deposit thicknesses in any of the tubes.

The second visual inspection of the new set of tubes was conducted on March 16, 1984, and showed no significant deposits build-up in any of the tubes. On May 18 and June 8, 1984, substantial deposits were observed in the tubes, and in the inlet and exit water boxes of the condenser.

The accumulated deposits in the untreated controlled segment of the inlet water box were greater than the deposits in the treated segments. On June 8, 1984, deposits were collected separately, from the exit water box and from the three segments of the inlet water box, for chemical analysis. In these inspections no tubes were removed.

On June 30, 1984, a retubing crew from Florida Power assisted the University in the tube removal. It was decided to remove Tube #1 (LKC), Tube #6 (untreated), tubes #9 and #12 (HYDRODYNAMIC/ TURGOMAG). Measurement of deposit thicknesses were made for two specimens from each tube. The results of these measurements and chemical analyses are discussed below.

On August 7, 1984, testing was ended, however, at that time it was decided to check the tubes, with the aid of an electron ultrasound detector, for any physical damage, such as corrosion, pitting, etc. The results of this test showed no physical damage to any of these tubes, except Tube #1. It was believed that Tube #1 was damaged prior to any testing. All tubes were then removed from the condenser, and deposit thickness measurements and chemical analyses were performed.

Deposit Thickness

The technique used in the measurement of the deposit thickness was described in a previous paragraph. In this section, the results of these measurements will be discussed in detail. Table 1 presents the results of deposit thickness measurements for tubes, which were tested for six months, beginning January 16, 1984, and ending June 30, 1984.

TABLE 1

THE AVERAGE THICKNESS OF THE DEPOSITS

JUNE 30, 1984 SIX MONTHS

	Ave. thickness of the deposits in Sample A "mm"	Ave. thickness of the deposits in Sample B "mm"	Total ave. of the thickness in Sample A & B "mm"	Total ave. of the thickness of the deposits in tube #9 & #12 "mm"
Tube #1 Treatment LKC	.5409	.3605	.4326	
Tube #6 Untreated	.4938	.47025	.4860	
Tube #9 *received treatment from Turbomag/PUM	.5585	.5614	.560	
Tube #12 *received treatment from Turbomag/PUM	.7349	.4154	.5979	.577

This table shows that one tube was chosen from each of two sections, and two tubes were chosen from the third section to measure deposit thickness. The tubes chosen were #1 (LKC), #6 (untreated), and #9 and #12 (Hydrodynamic/Turbomag).

Two specimens were then cut from each tube, and labeled A and B. The average thickness of the deposits, from each sample, were measured and recorded. Furthermore, the average thickness of samples A and B, for each tube, were calculated for their total average thickness, and the total average thickness for tubes #9 and #12 were averaged togethe to get their final total average thickness.

From this table, it is observed that there is a great amount of variation in the deposit thicknesses in each sample. Based on these observations, there is not enough evidence to conclude that deposit thickness is significantly affected by the magnetic treatment.

Table 2 shows the results of deposit thickness measurement for tubes which had not been removed during the June 30, 1984, inspection. These tubes were under test for a period of seven and one-half months, beginning January 16, 1984, and ending August 7, 1984. These tubes were #2, #3, and #4 (LKC), #5, #7, and #8 (untreated), and #10 and #11 (Turbomag/Hydrodynamic). From all the tubes listed above, only one specimen was taken from each. The total average thickness of the deposits was then calculated for each set of tubes. The observed results of the total average thickness

TABLE 2

THE AVERAGE THICKNESS OF THE DEPOSITS

AUGUST 07, 1984 APPROXIMATE PERIOD

OF TIME SEVEN AND ONE-HALF MONTHS LKC TREATMENT

TABLE B, LKC TREATMENT

Ave. thickness of the deposits in tube #2 "mm"	Ave. thickness of the deposits in tube #3 "mm"	Ave. thickness of the deposits in tube #4 "mm"	Total ave. thickness of the deposits in tubes #2, 3, 4 "mm"
.7760	.533	1.0112	.7734

TUBES THAT RECEIVED UNTREATED WATER B1

Ave. thickness of the deposits in tube #5 "mm"	Ave. thickness of the deposits in tube #7 "mm"	Ave. thickness of the deposits in tube #8 "mm"	Total ave. thickness of the deposits in tubes #5, 7, 8 "mm"
1.01126	.9720	1.29	1.0342

TUBES THAT RECEIVED TREATED WATER FROM

THE TURBOMAG AND THE PERMENANT UNIT MAGNET

TABLE B2

Ave. thickness of the deposits in tube #10 "mm"	Ave. thickness of the deposits in tube #11 "mm"	Total ave. thickness of the deposits in tubes #10, 11 "mm"
.9171	.4467	.6819

of the deposit in tubes which received untreated water, was approximately 1.0mm, whereas the deposit in tubes which received LKC treated water was approximately .77mm, and the deposit in tubes which received both Turbomag and Hydrodynamic treated water was approximately .68mm. In spite of the large variation in deposit thicknesses in each sample, the results show that the magnetic treatment reduces the average amount of deposits on the tube surfaces.

Table 3 shows the results of the average thickness of deposits, for a new set of tubes (#1, #6, #9 and #12) which were installed during the period from June 30, 1984, to August 7, 1984. These tubes had been under test for approximately one and one-half months. The average thickness of these deposits was measured using one sample from each tube. The average thickness of the deposits in tubes which received LKC treated water was approximately .28mm, and the tubes which received Hydrodynamic treated water was approximately .40mm, whereas the tube which received untreated water had a deposit thickness of approximately .53mm.

Analysis of the total average thickness of the deposits in tubes which received untreated water leads the observer to the following conclusion. The accumulation of deposits for the one and one-half months of testing, were equal to deposits accumulated during the first six months of testing. In addition, it can be observed that if the total average thickness of deposits in Table 2 were subtracted from the total average thickness of deposits in

TABLE 3

THE AVERAGE THICKNESS OF THE DEPOSITS

PERIOD OF TIME: JUNE 30, 1984 TO AUGUST 07, 1984

Ave. thickness of the deposits in tube #1 'LKC Treatment' "mm"	Ave. thickness of the deposits in tube #6 'Untreated' "mm"	Ave. thickness of the deposits in tube #9 'Only perm. unit magnet' "mm"	Ave. thickness of the deposits in tubes #12 'Only Perm. unit MAG' "mm"	Total ave. thickness of the deposit in tubes #9, 12 "mm"
.2821 mm	.5252	.3213	.4860	.4036

Table 1, the results would be equal to the average thickness of deposits in Table 3. These observations reveal that the rate of deposition in the summer was greater than in winter. This was attributed to the increase of cooling water temperature, and to the increased rate of bacteria growth.

Also, a careful examination of the total average thickness of deposits in tubes which received treated water from the LKC unit, leads the observer to the following conclusion. The accumulated deposits in the final one and one-half months were less than the deposits accumulated during the first six months of testing. In addition, it can be observed that, if the total average thickness of deposits in Table 2 were subtracted from the total average thickness of deposits in Table 1, the results would be approximately equal to the average thickness of deposits in Table 3. This conclusion indicates that the magnetic treatment is more effective with warmer saltwater. Furthermore, the above observations will encourage the researcher to deduce that if magnetic energy is added to a system, it will increase the activation energy of atoms. The increase in activation energy will lead to a decrease in the diffusion rate between atoms.

Quantitative comparison between the total average thickness of deposits that were scraped from tubes which received treated water from the Turbomag and Hydrodynamic units simultaneously, shown in tables 1 and 2, showed no sigificant difference. However, the total average thickness of deposits in tubes which received treated water only from the Hydrodynamic unit that had been under test for one and one-half months were significantly less than those accumulated in the initial six months. This is also an indication that the magnetic treatment is more effective in warmer water. In addition, the decrease in the average amount of deposits during summer time reveal to the researcher that the magnetic energy will slow the diffusion process between the atoms.

Finally, a heat transfer rate analysis was performed on this condenser. Dr. Hosler, Professor in the Mechanical Engineering Department at the University of Central Florida, ran this analysis. Dr. Hosler's conclusion is, "With increasing deposit build-up, treated and untreated water would approach similar reduction in heat transfer".[15]

Chemical Analysis of Deposits Scraped from the Water Boxes

The chemical analysis of deposits scraped from the water boxes were performed by University of Florida personnel. In this analysis, samples were taken from each of the three sections of the inlet water box, and the exit water box. To analyze these deposits, Energy Dispersive Spectrometry (EDS) was used to determine qualitatively the coexisting elements; whereas, quantitative measurements are not possible by using EDS.

The EDS results shows that silicon, phosphorous, chlorine, potassium, calcium, copper, iron and zinc were the elements contained in the deposits. The data, obtained by the EDS, indicated that iron and chlorine were the major constitutents among the other elements.

By using a diffractometer, the compounds contained in the samples were determined and listed below:

Sample 1 - Inlet - LKC Treated Water
Principal compound FeO(OH)

Sample 2 - Inlet - Untreated Water
Principal compounds FeO(OH) and FeO

Sample 3 - Inlet - Turbomag/Hydrodynamic Treated Water
Principal compounds FeO(OH) and FeO

Sample 4 - Outlet
Principal compound FeO

All the chemical compounds are iron oxide compounds.

Chemical Analysis of Deposits Scraped from Condenser's Tubes

The method described above in analyzing the deposits in the water boxes was used to analyze the deposits scraped from tubes that were removed on June 30, 1984. This analysis was also performed by University of Florida personnel.

The conclusion concerning this analysis was stated as follows: "The chemical nature of the deposits was not affected by the magnetic water treatment. Therefore, it does not appear that the magnetic treatment would reduce the degree of adherence or the amount of deposits."

The results of the analysis indicated that the elements present in these deposits are chlorine, silicon, sodium, calcium, iron and copper. However, it was determined that chlorine was the principal constituent. In addition, the analyzer was able to identify the coexisting compounds in these deposits. The results indicated the following compounds:

Tube #1 - LKC Water Treatment
Principal compounds NaCL and Calcite (CaCo)

Tube #6 - Untreated Water
Principal compounds NaCL and Calcite

Tube #9 - Hydrodynamics Treatment
Principal compound NaCL

It can be observed that the elemental and compound analysis of the deposits in the tubes numbered above are the same.

Conclusion

The conducted experiment was ended on August 7, 1984. During the time of operation, three differently designed magnetic units were under test. These units were the Linear Kinetic Cell, the Turbomag Unit, and the Hydrodynamic Unit. Since the Turbomag Unit was noisy during its operation, and required more maintenance work, it was replaced by the hydrodynamic unit in the final stage of testing. They were placed in a position to evaluate their effectiveness on the seawater used to cool a condenser operating at temperatures typical of power plant condensers.

The chemical analysis and the thickness measurement of deposits collected from tubes which received treated and untreated water showed similar results. Even though there is some difference in deposit thicknesses, it does not appear to be significant in terms of heat transfer. Since the use of three different magnetic devices had physically affected the deposits in similar fashion, it appears that the method of producing the magnetic field is not of primary importance.

The magnetic treatment has affected the deposits in the following manner: it slightly reduced their degree or adherence and it changed the physical structure of the deposits. In summary, the use of a magnetic device would not affect the method of tube cleaning, especially in the long term.

LITERATURE SURVEY

Introduction

The main purpose of this survey is to achieve a theoretical understanding concerning four subjects: the kinetics of phase transformations, homogeneous nucleation, rate of nucleation, and the growth of a nucleus. These topics will provide greater insight concerning the size, shape, formation, number, rate, and growth of nuclei.

The mathematical equations supporting each of these topics are based on information developed in other studies. These studies involve crystal imperfection, diffusion process, and reaction rate theory.

Additional information also has been provided relating to atomic modeling, electron affinity, interatomic forces, and atom arrangements. This background is necessary as a guide to help explain the physical structure of crystals.

Atomic Modeling and Energy Levels

An atom is visualized as being composed of a positively in charged nucleus with orbiting electrons [1]. Bohr assumed that when an electron moves from one orbit to another, a specific amount of energy would be absorbed or emitted. This theory was verified by experiments that he conducted in 1913.

The hydrogen atom is the simplest known element and is composed of one electron and one proton. Bohr had considered this simple element in order to derive the energy equation of an atom, assuming that the proton is not moving, and the electron is in a circular orbit about the proton. Bohr stated that to form an atom a force must exist to hold the electron and the proton together. This attractive force is the coulomb force. In addition, energies are associated with these forces. These energies are the potential and the kinetic energies. Therefore, the total energy of the atom is given as:

$$E = PE + KE$$

where E is the total energy of an atom, PE is the potential energy and KE is the kinetic energy.

First, the potential energy term will be derived. Consider two charged particles, namely, a proton and and electron. Assume that the potential energy of these particles is zero when they are at an infinite distance from each other (Figure 4). To form an atom, the electron must move toward the proton. During this transition period work is done by the coulomb force. Thus

$$PE = \int_{\infty}^{r''} F dr \qquad (1-1)$$

where r' is the distance between the proton and the electron as they approach each other, r'' is the final separation distance between the two particles, and F is the Coulomb force.

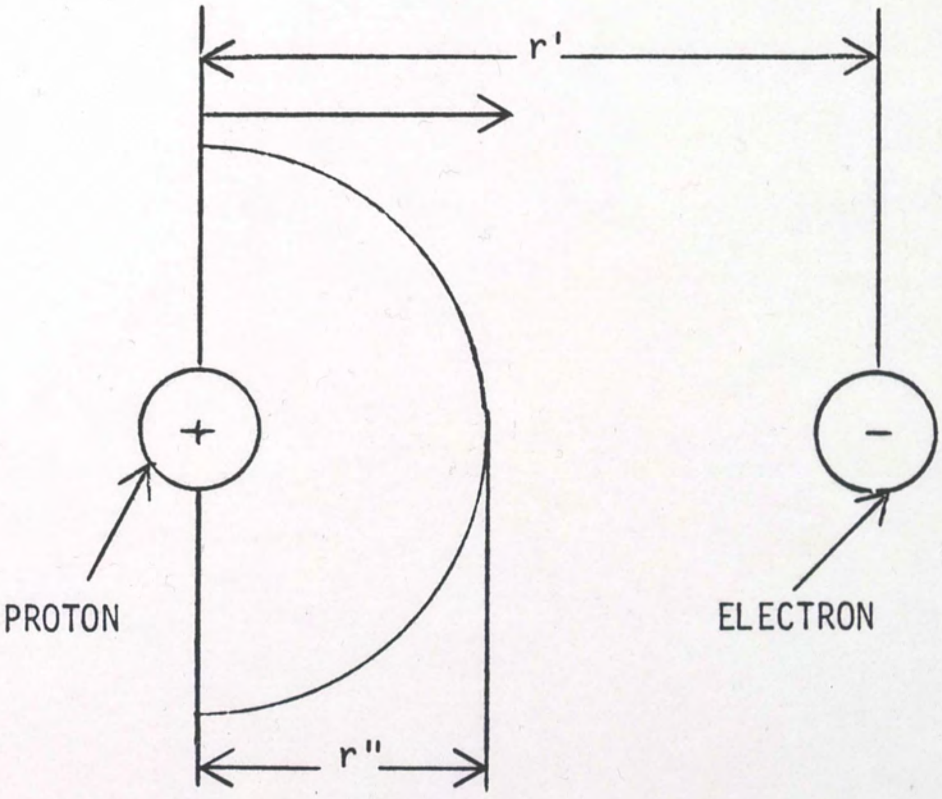

FIGURE 4. A PROTON AND AN ELECTRON SEPARATED BY AN INFINITE DISTANCE BETWEEN EACH OTHER.

From elementary physics, the mathematical form of the Coulomb force is given as:

$$F = -q_1 \times q_2/r'^2 \qquad (1\text{-}2)$$

where q_1 is the charge of the first particle and q_2 is the charge of the second particle. The two charges, q_1 and q_2, will be replaced by another symbol, e. These two charged particles are the electron and the proton. The electron is designated as a negative charge (its charge = $-e$) whereas the proton is designated as a positive charge (its charge = $+e$). Therefore, Equation 1-2 could be written as:

$$F = -(-e \times e)/r'^2 = e^2/r'^2 \qquad (1\text{-}3)$$

substituting Equation 1-3 into Equation 1-1 and integrating, the result will be:

$$PE = \int_{\infty}^{r''} e^2/r'^2 dr' = -e^2/r'' \qquad (1\text{-}4)$$

Second, the kinetic energy term will be derived. As was mentioned before, the electron of mass m is moving in a circular orbit around the proton (Figure 5). Its acceleration "a" is centripetal, directed constantly toward the center of the circle

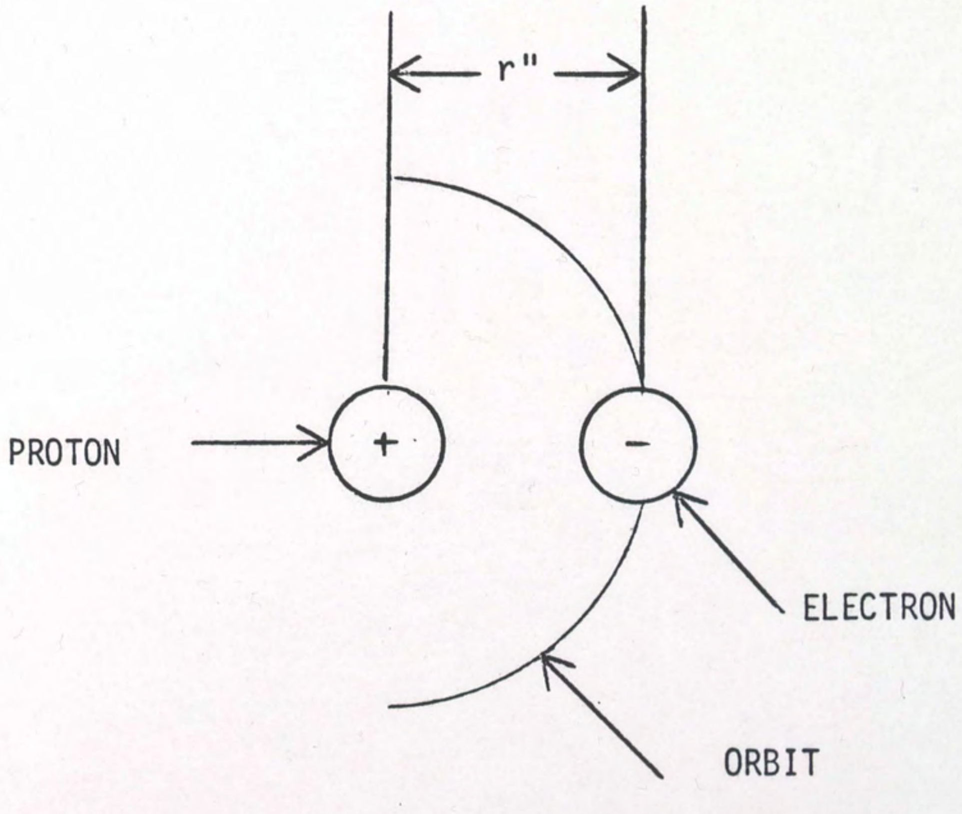

FIGURE 5. AN ELECTRON ORBITING A PROTON IN A CIRCULAR ORBIT WITH RADIUS r".

such that

$$a = v^2/r' \tag{1-5}$$

where v is the velocity of the electron.

According to the fundamental relation of the dynamics of a particle, the existance of the acceleration implies the existence of a corresponding force, applied on the particle, such that

$$F = ma \tag{1-6}$$

Substituting equations 1-2 and 1-5 into Equation 1-6 results in:

$$e^2/r''^2 = mv^2/r'' \tag{1-7}$$

or

$$mv^2 2 = e^2/2r'' = KE \tag{1-8}$$

Therefore, the total energy of the hydrogen atom is

$$E = -e^2/r'' + e^2/r'' = -e^2/2r'' \tag{1-9}$$

Equation 1-9 is called the Bohr's energy equation of the hydrogen atom. It shows that as the orbit radius decreases, the energy of the atom decreases. in addition, it is noted, in many material science references [2], that the smallest radius of an electron is .528 Angstron (A) where 1A = 10 -8cm. The other allowed radii are expressed in terms of the smallest, thus:

$$r" = -n^2/r_1 \qquad (1\text{-}10)$$

$n = 1,2,3,4,5,6...$

$rl = .528A$

where r"n are the allowed radii which corresponds to the interger n. Substituting Equation 1-10 into 1-9, the energy equation of the allowed radii orbit can be found as:

$$E = -e^2/2n^2 \text{ x } r_1 \qquad (1\text{-}11)$$

Equation 1-11 indicates that energy is quantitized. Also, it shows that n tends to go to infinity and E tends to go to zero. Furthermore, it implies that the electron is attached at the boundary of the atom, and it takes energy to remove the electron or ionize the atom.

Electron Affinity and Ionization Energy

The ionization energy is the energy required to remove the tightly bound electron from an atom [2]. Both the ionization energy and the electron affinity are responsible in forming positive and negative ions from neutral atoms. Mathematically, the ionization energy is expressed in the following manner:

$$E_{ion} = E_{final} - E_{initial}$$

A positive quantity of the ionization energy means that energy must be added to the atom in order to form an ion. Since ionization depends on initial distance between the electron and the proton, large atoms will have a lower ionization energy than small atoms.

Now, when an electron is captured by an atom, there is an energy release. This process is exothermic and resuts in the formation of a negative ion; this phenomena is called the electro affinity of an atom.

Interatomic Forces

The interatomic forces are grouped into two categories.[3] First, large interatomic forces result in a strong bond between atoms. Those are the ionic, covalent, and metalic bonds. Second, small interatomic forces result in weak bonds. These are found in Van Der Waals and hydrogen-bonded substances.

Atom Arrangments

There are two basic models used in atom stacking. The first model used in stacking will generate a hexagonal close pack (HCP). The second model is ithe face centered cubic (FCC).

In the formation of these two models, the atoms are stacked in a way to minimize the open space between them. Figure 6 shows the smplest crystal structure, and is called the close-packed crystal structure, and this layer of atoms will be designated as the A-TYPE layer. To build up the three dimensional close-packed structure, another two layers of this type will be placed on top of one another in a systematic fashion as shown in Figure 7.

The A-TYPE layer of atoms is in a plane parallel to the viewer's sight. The second layer of atoms designated as the B or C-TYPES, are placed on top of the first layer, with the atoms of the B or C-TYPES fitting into one of the sets of hollows provided by the first layer, also referred to in Figure 7. At this stage, the structure is the same. However, the difference in stacking comes with the placing of the third layer of atoms. For all means and purposes, considering the B-TYPE configuration the third layer could be placed over the hollows of the first layer, i.e., another layer of A-TYPE, Figure 8. It also could be placed over the hollow that is not over the first layer, i.e., a C-TYPE layer, Figure 9.

These two basic stackings are known as the ABABAB stacking model which generate the hexagonal close-packed (HCP), Figure 10, and the ABCABC stacking model which generate the face-centered-cubic (FCC), Figure 11.

The sites in between the atoms will be referred to as interstices. For the close-packed structure, there are two major

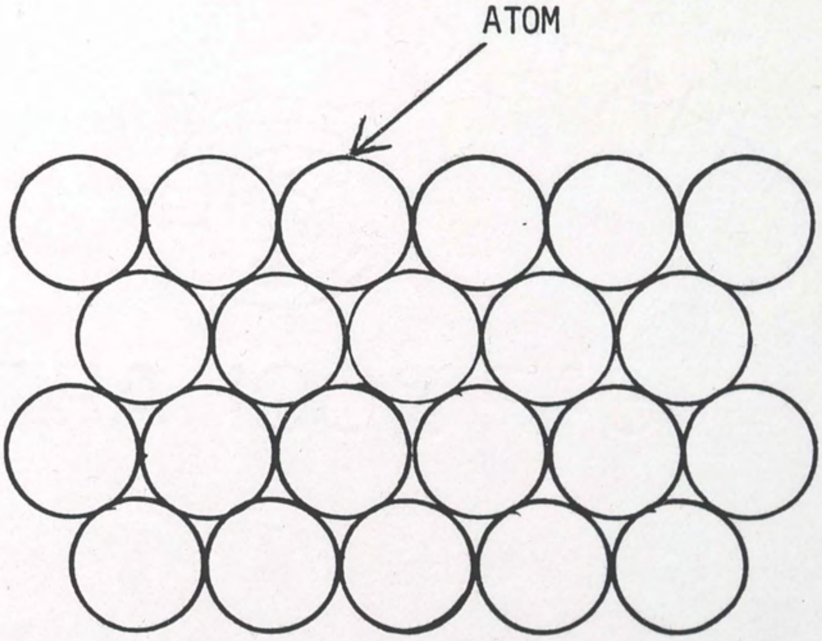

FIGURE 6. CLOSE-PACKED LAYER OF ATOMS.

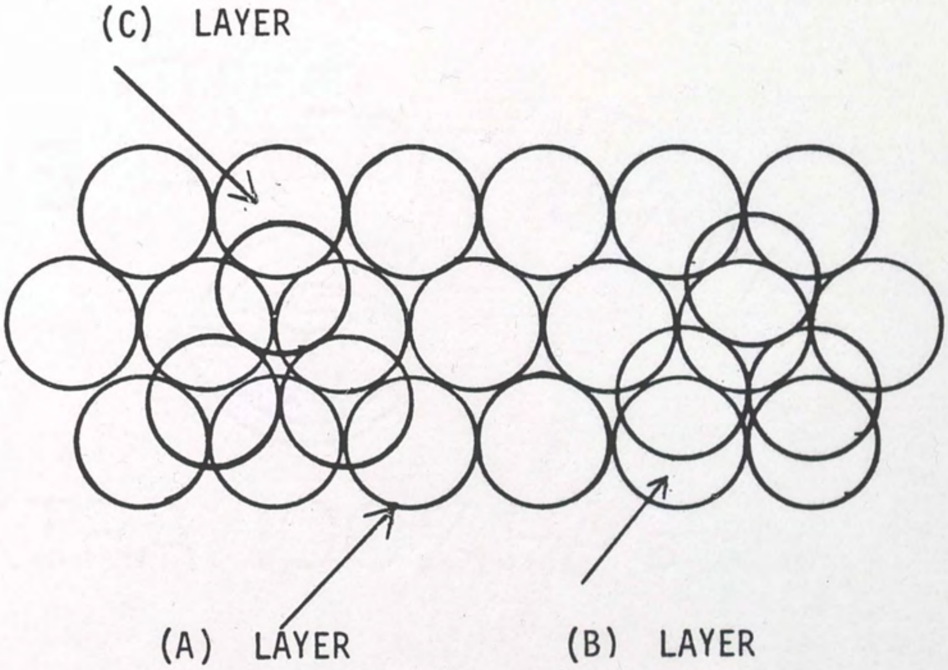

FIGURE 7. STACKING OF TWO CLOSE-PACKED LAYER.

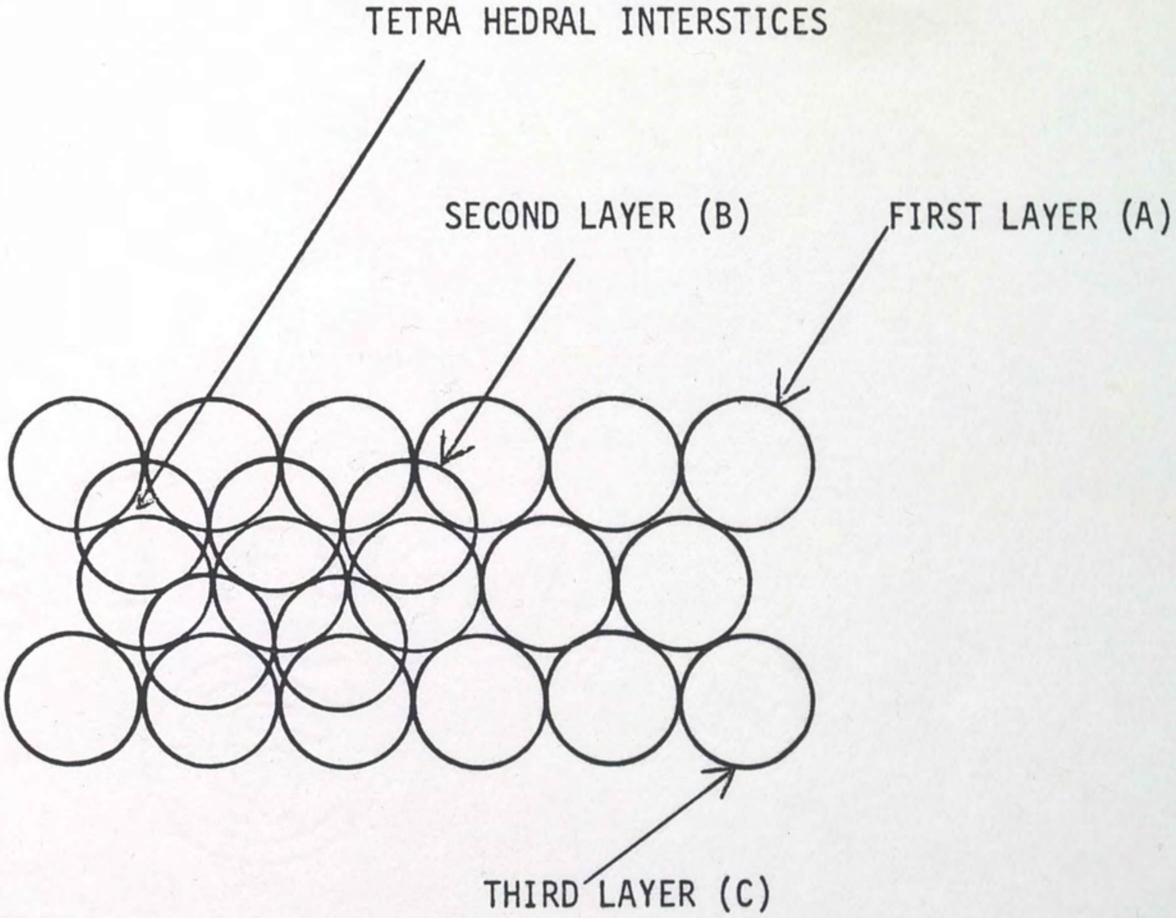

FIGURE 8. PACKING OF ATOMS IN A HCP MODEL.

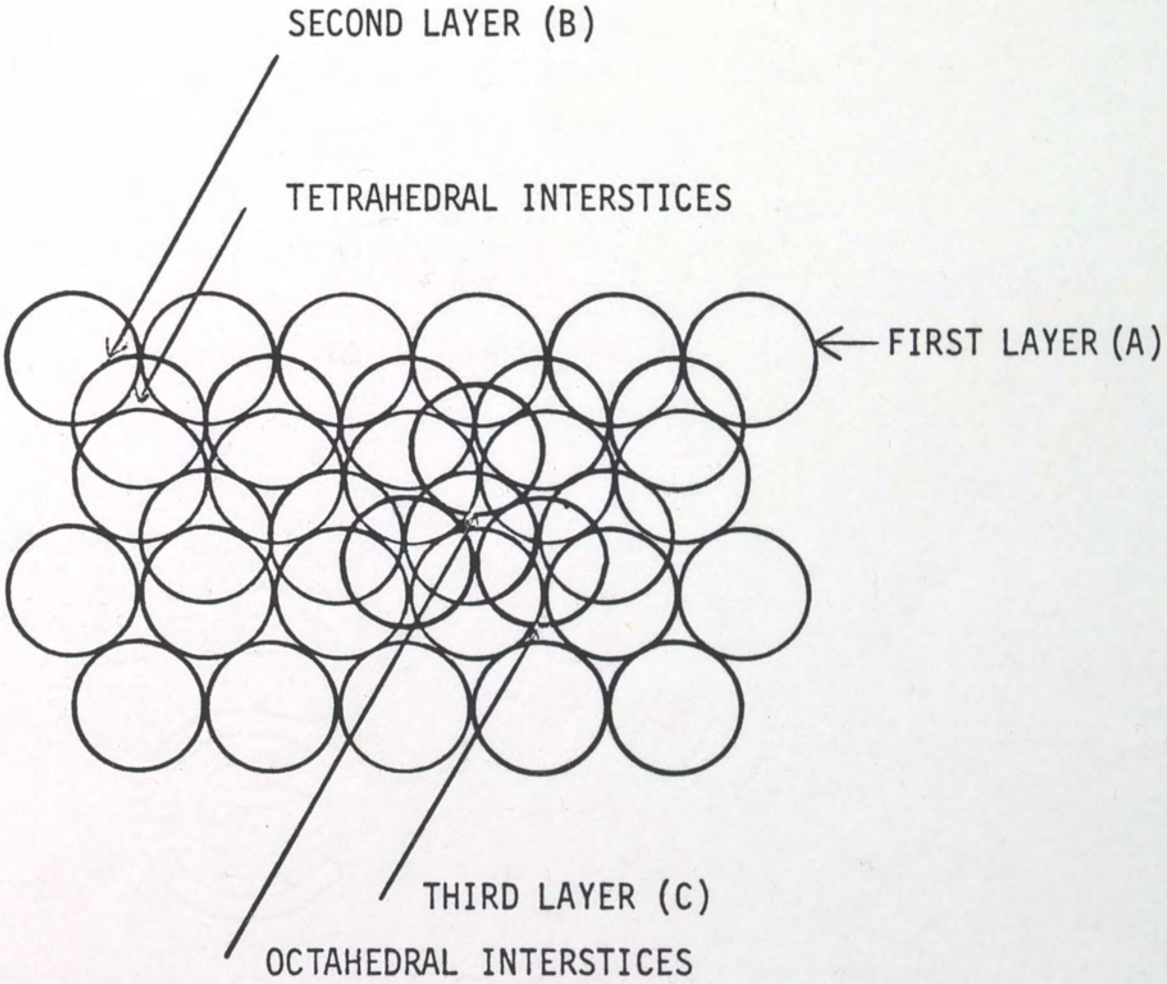

FIGURE 9. PACKING OF ATOMS IN A FCC MODEL.

FIGURE 10. HEXAGONAL CLOSE-PACKED UNIT CELLS.

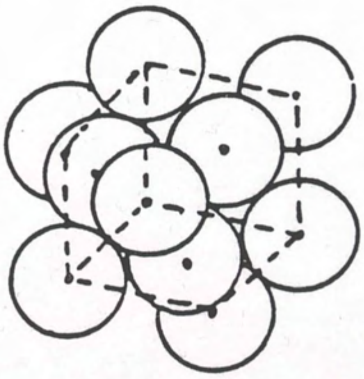

FIGURE 11. FACE-CENTERED CUBIC UNIT CELLS.

kinds of interstices, those are the tetrahedral sites having four nearest neighbor atoms and the octahedral sites having six nearest neighbor atoms.

Imperfections in Crystals

Previously, the structure of a crystal was described as an (HCP) and (FCC) models [4]. Since crystalline solids found in nature do not quite have the perfect symmetry of ideal crystals, they contain structural imperfections which affect their mechanical properties. The imperfections exist at the atomic level.

A point defect in a crystal is an example of an imperfection. This defect has a significant effect on diffusion and mechanical properties.

There are two types of point imperfections, the vacancy type, and the interstitial type, Figure 12. A vacancy is caused by an atom not appearing at an atom site; the interstitial is caused by an atom taking up residence in a space between lattice sites as seen in Figure 12.

To calculate the number of vacancies or interstitials, the first and second law of thermodynamics will be applied to a crystal. Consider a crystal, with given temperature and volume, where the free energy is a minimum and the crystal is in its most stable state. (i.e., no further physical change will occur in a crystal when energy is added or taken.) Mathematically, the above thermodynamic laws are expressed as:

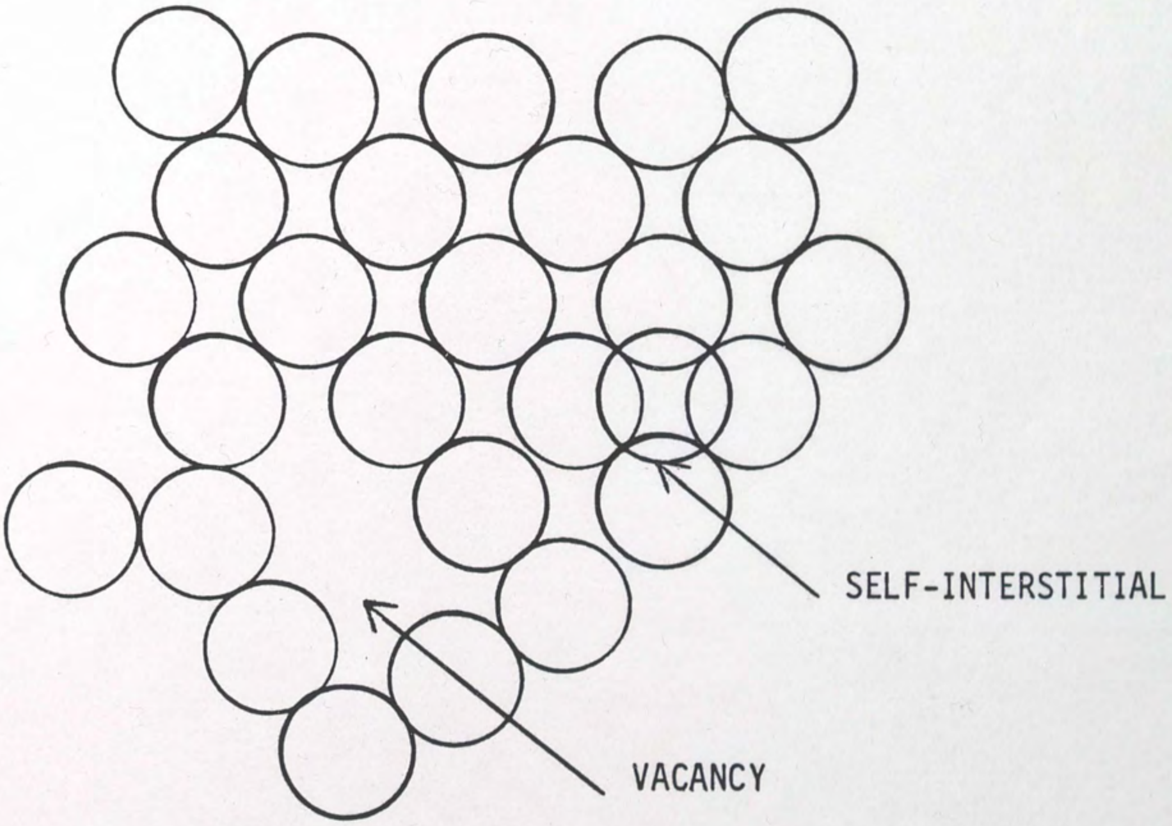

FIGURE 12. POINT DEFECTS IN A CRYSTAL SHOWING A VACANCY AND A SELF-INTERSTITIAL.

$$\Delta G = \Delta E - \Delta Q \tag{1-12}$$

$$\Delta Q = T\Delta S \tag{1-13}$$

$$\Delta G = \Delta E - T\Delta S \tag{1-14}$$

where G is the free energy change, E is the internal energy change or bond energy change, and $T\Delta S$ is the mixing energy change. The difficulty of this problem is to find the number of vacancies corresponding to the minimum value of ΔG. For a crystal at a constant temperature, the amount of disorder or the entropy in a crystal will increase gradually as vacancies are introduced into a perfect lattice; which means that the quantity $T\Delta S$ is increased as the number of vacancies increase. As the term $T\Delta S$ increases, the free energy tends to decrease. Thus, in order to create a vacancy, an atom must be removed from a lattice site. For that to happen, it requires bonds breakage between the atoms. In addition, energy must be added to the crystal to create a vacancy, and the number of these vacancies in a crystal will correspond to the minimum free energy.

To find the equilibrium number of vacancies, the internal energy and the mixing energy must be expressed in terms of the number of vacancies. The derivation, in finding the equilibrium number of vacancies, can be accomplished by using statistical thermodynamics [1]. The final results obtained are:

$$N_v/N = \exp(-\Delta E/KT)$$

where N_v is the number of vacancies in a crystal, N is the number of lattice sites in a crystal, ΔE is the energy required to form a vacancy or the internal energy, K, is the Boltzmann's constant, and T is the absolute temperature of a crystal.

Reaction Rate Theory

The description of atom motion, Figure 13, could be best described from the reaction rate theory [5]. The motion of an atom from one position to another will be postulated in terms of an activated state with a definite activation free energy.

In order for the vibrating atom at Position "A" to move to Position "C," it must surmount the energy barrier at Positon "B." Thus, a free energy must be supplied to the atom and this thermal free energy is equal to $G_b - G_a$, and it is in the form of atomic vibration.

From the statistical thermodynamic point of view, the probability, p, that an atom will gain enough thermal energy to surmound a barrier of ΔG^*, which is equal to $G_b - G_a$, is given as:

$$P = \exp(-\Delta G^*/KT) \qquad (1\text{-}16)$$

In addition, the rate, R, at which the atom surmounts the barrier of

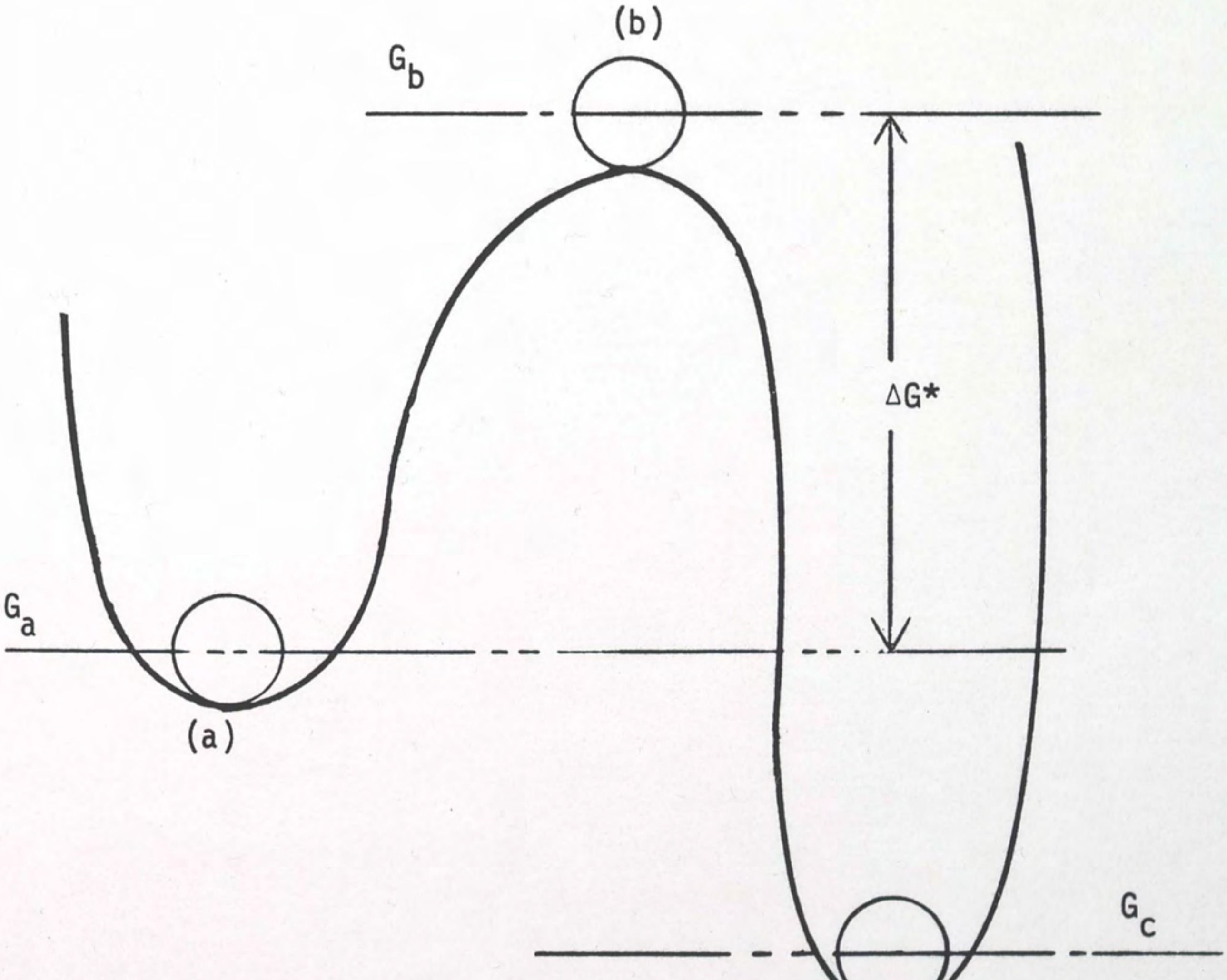

FIGURE 13. DESCRIPTION OF AN ATOM MOTION FROM METASTABLE TO UNSTABLE THEN TO STABLE STATES.

height ΔG^* is given as:

$$R = U \times \exp(\Delta G^*/KT) \qquad (1\text{-}17)$$

where U is the frequency with which an atom will attempt to surmound the barrier ΔG^*.

Introducing the star notation "*", Equation 1-14 could be written as
$\Delta G^* = \Delta E^* - T\Delta S^*$. Substituting Equation 1-14 into Equation 1-17:

$$R = U \times \exp(\Delta S^*/K)\exp(-\Delta E^*/KT) \qquad (1\text{-}18)$$

where ΔS^* is the entropy of activation, and ΔE^* is the internal energy of activation or the activation energy. Equation 1-18 is called the Arrhenius equation, and its general form is found as:

$$RATE = A \times \exp(-\Delta E^*/KT) \qquad (1\text{-}19)$$

where A is a constant for a particular process.

Arrhenius equation is one of the fundmental equations for understanding the movement of atoms in diffusion, oxidation and phase transformation.

Atomic Diffusion

Diffusion, on the atomic scale, is the net effect of random atomic motion. It is the mechanism by which matter is carried through matter. Also, one could think of diffusion as "the great randomizer" which erases all differences in concentration by random atomic motion. An example of a diffusion process is the diffusion of heat that occurs when one end of a bar is heated and the other ends warms up after time "t." Because diffusion occurs spontaneously, one must view the process as entropy increase which means a decrease in the free energy.

Mathematical Analysis of Diffusion

Consider solute atoms between two parallel atomic planes, Figure 14. These two planes are separated by a distance "a".[6] Also, assume that there are "C_1" solute atoms per volume on plane "1," and "C_2" solute atoms per volume on plane "2" where "C_1" is greater than "C_2." Therefore, the concentration gradient dc/dx = $(C_2-C_1)/a$ exist in the "x" direction.

Next, assume that "R_1" is the atomic jump frequency from each plane. Therefore, the net flux of diffusion solute atoms "J" from plane "1" to plane "2" is found as:

$$J = a(C_1 - C_2)R_1/2 \qquad (1\text{-}20)$$

where the factor ".5" accounts that atoms might jump in the positive

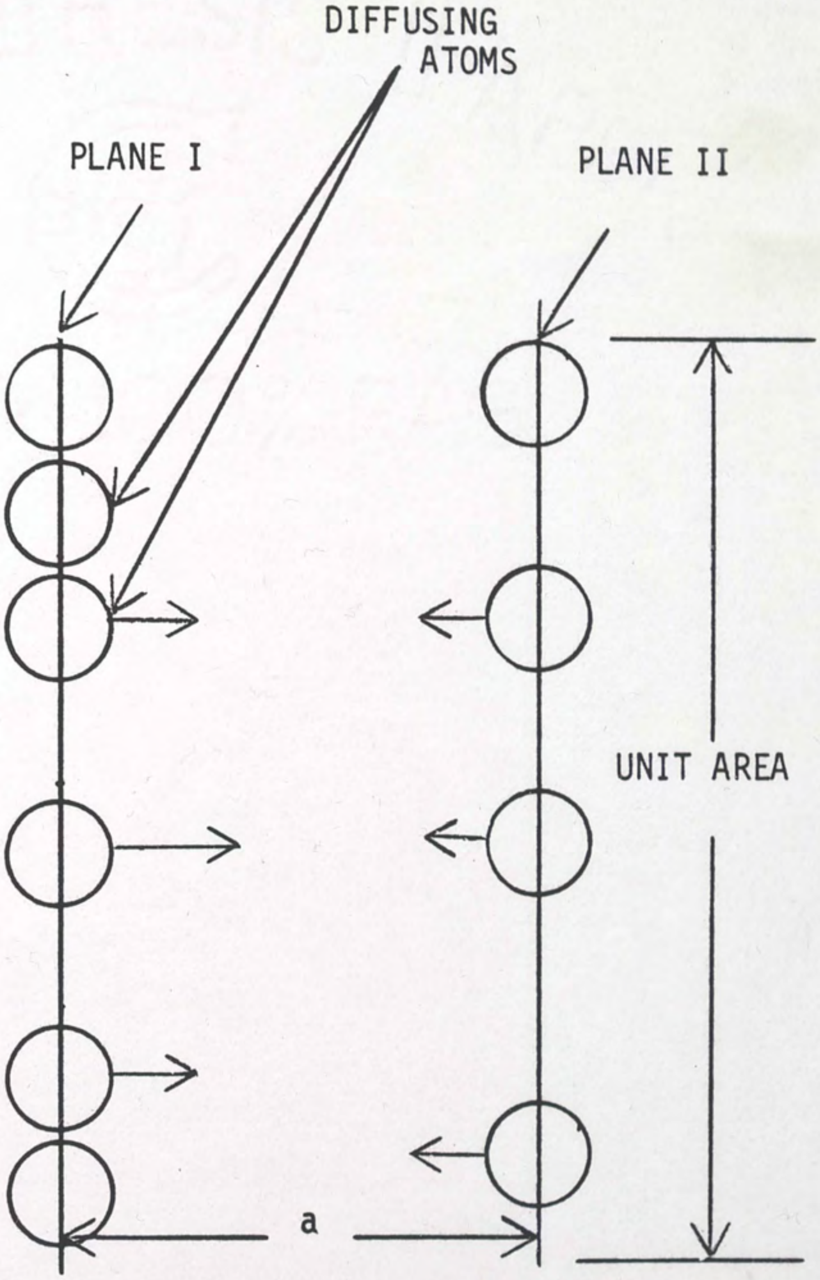

FIGURE 14. RELATION BETWEEN ATOMIC JUMPS AND DIFFUSION IN A CONCENTRATION GRADIENT.

"x" direction, or the negative "x" direction. Thus, by substituting dc/dx into Equation 1-20, the net flux could be written as:

$$J = \frac{a^2 R_1}{2}\,\frac{dc}{dx} \qquad (1\text{-}21)$$

or

$$J = \frac{-(a^2 R_1}{2}\,\frac{dc}{dx} = D\ dc/dx \qquad (1\text{-}22)$$

where $D = .5 \times a^2R_1\ \mathrm{cm}^2/\mathrm{sec}$ is the diffusion coefficient.

Equation 1-22 is known as Fick's first law of diffusion. If diffusion occurs in three dimensions, the value of the diffusion coefficient will differ by a actor of one-third, thus:

$$D = \frac{1}{6}\,a^2R_1 \qquad (1\text{-}23)$$

Substituting Equation 1-18 into Equation 1-23, the mathematical form of the diffusion coefficient will reduce to:

$$D = \frac{1}{6}\,a^2\ U \exp\left(\frac{\Delta S}{K}\right) \exp\,(-\Delta E/KT)$$

or

$$D = DO \times \exp(-\Delta E/KT) \qquad (1\text{-}24)$$

$$Do = 1/6\ a^2u \exp(\ S/K)$$

where the coefficient "DO" is independent of the temperature.

Self-diffusion most likely will occur by a vacancy mechanism, the interstitial mechanism will not be of primary importance to be discussed.

The Vacancy Mechanism

Consider a plane of atoms where a vacancy is provided for the shaded atom, Figure 15, to move into the vacancy.[7] As the atom starts to move to the right, there is a bond force to the left which tends to hinder its motion. Hence, the potential energy of the shaded atom will increase gradually from its initial position to overcome the retarding forces. This potential energy will reach a maximum when the shaded atom is in its midway motion, Figure 15. Further advancement of the shaded atom to the right will decrease the potential energy. Therefore, the potential energy of the atom is the same at both lattice positions, and it must surmount an energy barrier in order to move from one site to another. Two simultaneous events must occur when the solute or shaded atom moves to right. First, the atom must have sufficient energy equal to $\exp(-E_m/KT)$ to overcome a barrier energy; E_m is the activation

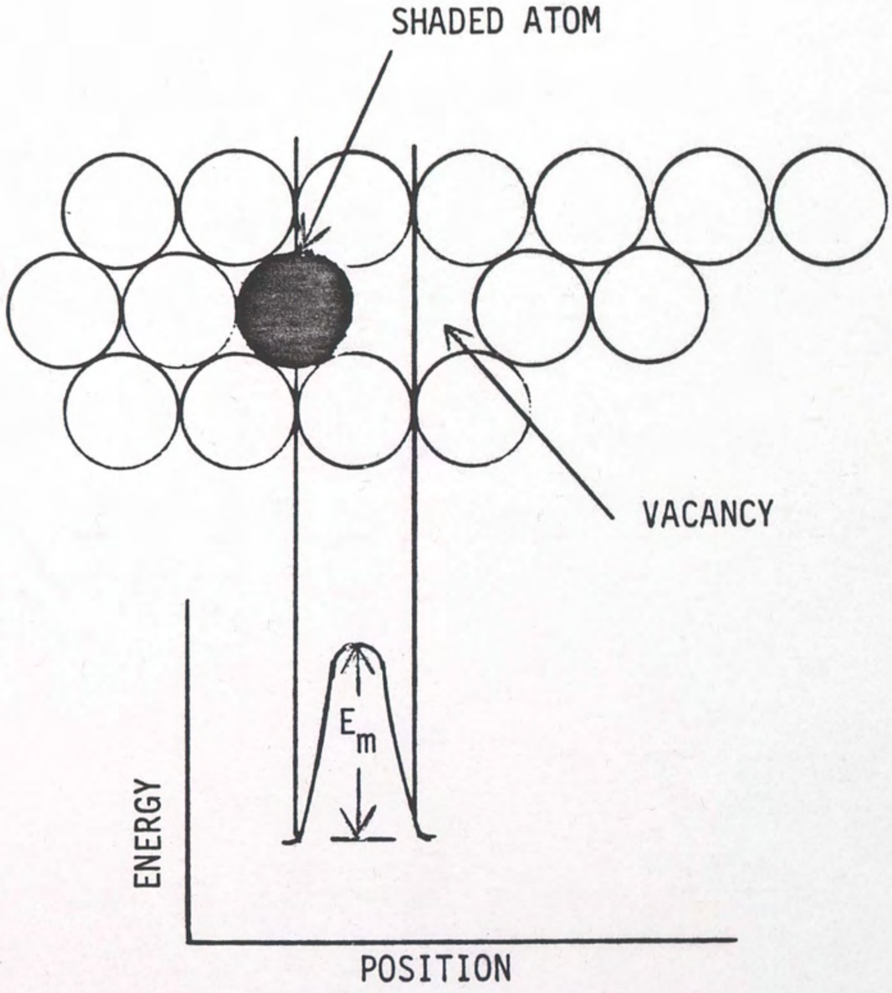

FIGURE 15. THE POTENTIAL ENERGY OF THE SHADED ATOM AS A FUNCTION OF POSITION.

energy for vacancy motion. Second, the energetic atom must have a vacancy next to it; the probability of this happening is equal to exp(E_v/KT) where E_v is the activation energy required to form a vacancy.

Therefore, the total activation energy for this vacancy controlled diffusion process is equal to exp[-(E_m+E_v)]/KT. In addition, it has been found through previous research and studies, that the activation energy for diffusion by a vacancy mechanism is greater than the activation energy for diffusion by interstitial mechanism.

Kinetics of Phase Changes

Materials processes such as solidification involve a change of phase[8]. The appearance of small particles of a new phase, in an old phase, will grow until the transformation is completed. The factors which are influenced by the phase change are the size, the shape, and the rate of formation.

Consider two phases α and β , Figure 16, where α phase is a liquid phase stable above a certain temperature T_e. The β phase is a solid phase stable below the temperature T_e which is the melting temperature. At $T=T_e$ the free energies of the two phases are equal, therefore $G_\alpha = G_\beta$ and the change in the free energy of the two phases is given as:

$$\Delta G_v = G_\alpha - G_\beta = 0 \qquad (1\text{-}16)$$

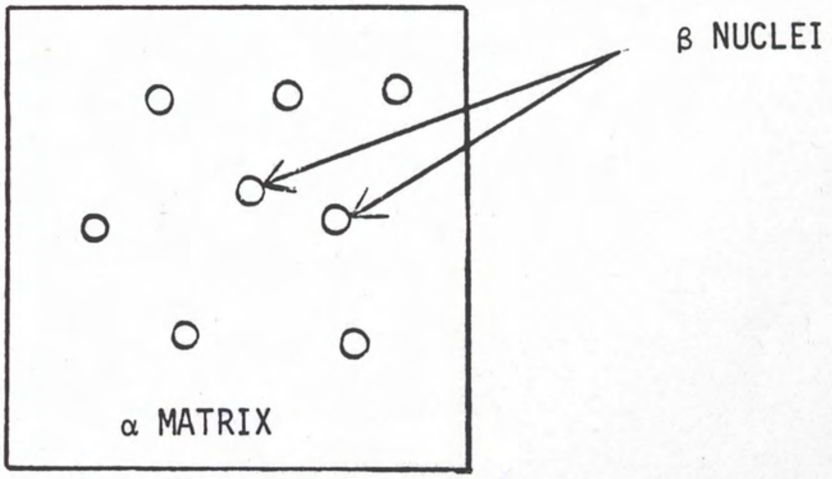

FIGURE 16. NUCLEATION.

where the subscript "v" indicates that energy is expressed per unit volume. Applying Equation 1-14 for the kinetics phase transformations, the results will be at $T = T_e$

$$\Delta G_v = \Delta E_v - T\Delta S_v = 0 \qquad (1\text{-}27)$$

$$\Delta S_v = \Delta E_v/T_e$$

At T not equal to T_e, the free energy is equal to

$$\Delta G_v = \Delta E_v - T(\Delta E_v/T_e)$$

or

$$\Delta G_v = (\Delta E_v)(\Delta T)/T_e \qquad (1\text{-}28)$$

Since solidification will occur when the β phase transforms to the phase, heat is evolved during this process which means that the internal energy change per unit volume is negative, as well as the free energy per unit volume. In addition, Equation 1-28 indicates that phase transformation is occurring, but it does not give information about the rate at which this transformation takes place. Furthermore, the formation of the β phase does not happen instantaneously. For the phase to form requires that atoms align themselves in specific position in the β lattice, which means that some local rearrangement is required. These atomic rearrangements are diffusion controlled processes. Therefore, the transformation from α to β phase is divided into two steps: nucleation and growth of nuclei.

Homogeneous Nucleation

The definition of homogeneous nucleation can be stated as the formation of many β nuclei. The average size of these β phases are very small [9]. In addition, the appearance of the β phase in the phase is accompanied by a decrease in the free energy.

Consider the formation of a small spherical β nucleus in the α phase. When the formation of the β nucleus is completed, the interface energy γ between the α and the β phase will be created. This γ is the surface free energy per unit area, and it is always positive since energy is always expended in making an interface.

The transformation of the α to the β form will be accompanied by a change in the bulk-free energy ΔG_v. Thus, the total free energy ΔG_t involved in making a spherical nucleus of radius r, is

$$G_t = \Delta G_t = \frac{4}{3} \pi r^3 \Delta G_v + 4\pi r^2 \gamma \tag{1-29}$$

The graphical interpretation, Figure 17, of the above

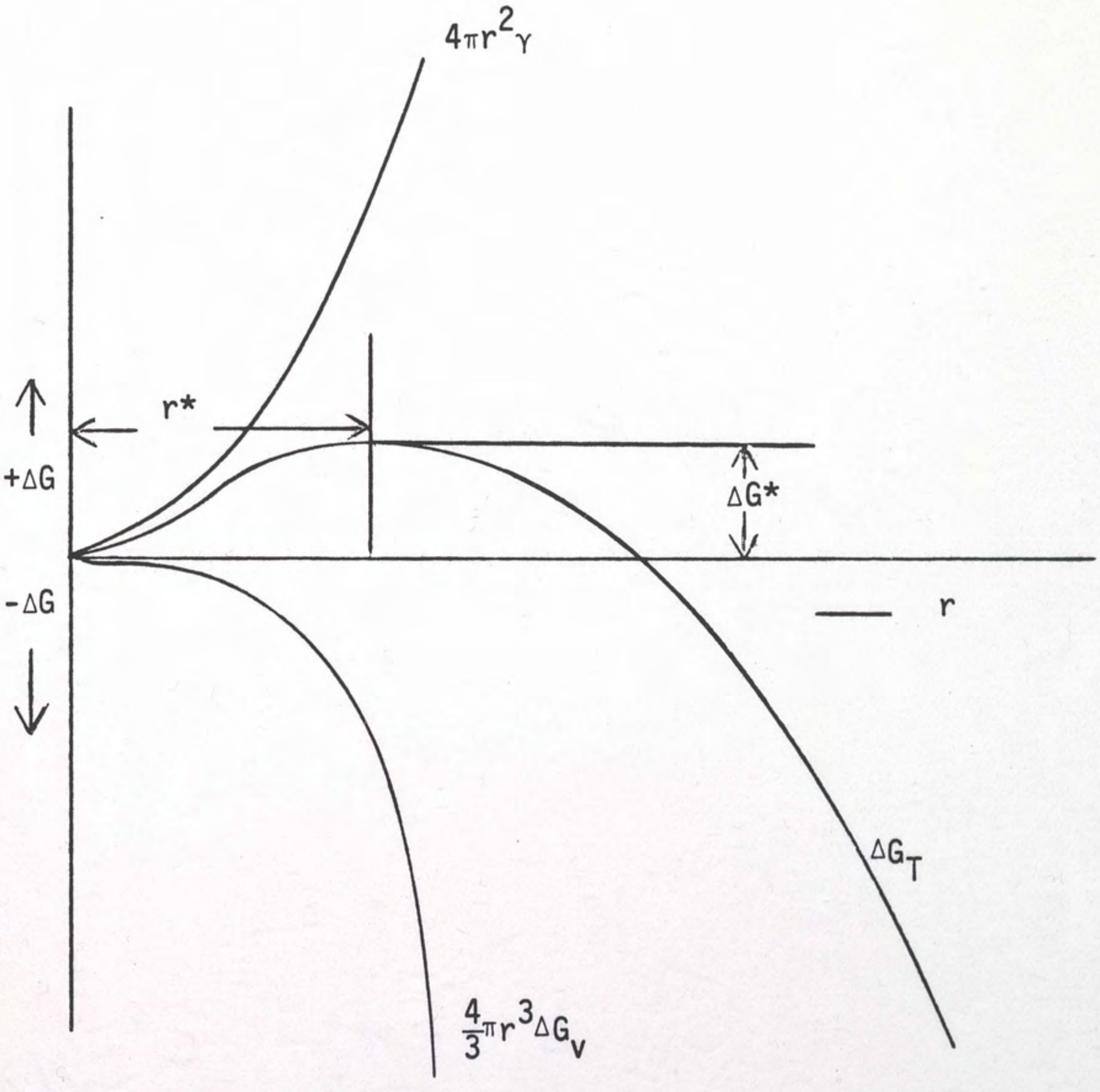

FIGURE 17. NUCLEATION OF SPHERICAL SOLID NUCLEI.

equation concludes that, as the spherical nucleus starts to appear, its free energy will increase until the critical radius r^* is reached. Therefore, when the radius r is less than the critical radius r^*, the surface term will dominate and ΔG_t increases with r which means that particles with radius less than r^* will tend to redissolve, and these particles are called embryos. However, particles with radius r greater than the critical radius r^* the volume term will dominate, and ΔG_t decreases rapidly with increasing r, under this condition the particle tends to grow and continue to grow with a decrease in the free energy. Particles with radius r greater than r^* are called nuclei.

When nuclei are formed, they must surmount a barrier energy. This energy is the critical total energy or the maximum value of ΔG_t which is equal to ΔG^*. The computation of ΔG^* is obtained by taking the derivative of ΔG_t with respect to r and setting ΔG_t equal to zero. Thus,

$$\frac{d}{dr}\left(\frac{4\pi\, r^3}{3}\right) \Delta G_v + \frac{d}{dr}\,(4\pi r^3)\,\gamma = 0 \qquad (1\text{-}30)$$

$$4\pi r^* \,\Delta G_v = -8\pi\ \gamma \qquad (1\text{-}31)$$

solving for r^*, the result is

$$r^1 = \frac{-2\gamma}{\Delta D_V} \tag{1-32}$$

substitute Equation 1-32 into Equation 1-29, the value of ΔG^* is obtained.

$$\Delta G^* = 4\pi\left(\frac{-2\gamma}{\Delta G_V}\right)^3 \frac{\Delta G_V}{3} + 4\pi\left(\frac{-2\gamma}{\Delta G_V}\right)^2 \gamma$$

after some manipulation, the value of ΔG^* is:

$$\Delta G = \frac{16\pi\ \gamma^3}{3(\Delta G_V)^2} \tag{1-33}$$

So far, only the equilibrium distribution of a nuclei has been considered. The rate and the growth of a nucleus are the target of the following discussion.

Rate of Nucleation

There are two major steps in the formaton of a stable nucleus. First, the nucleus must surmount the energy barrier ΔG^* [10]. Second, the atoms must diffuse and rearrange themselves to form a nucleus. Therefore, the rate of nucleation will depend on the number of nuclei which have sufficient energy to surmount the barrier energy and it will depend on the ability of atoms to diffuse into a nucleus. Mathematically, the rate of nucleation, N, is found as:

$$N = m \times \exp(-\Delta G^{*}/KT)\exp(-\Delta E/KT) \qquad (1\text{-}34)$$

where m is a geometrical constant and depends on the shape and size of the nucleus.

Growth of a Nucleus

After a nucleus appears it will reduce its total free energy,[11] and its growth will be considered stable at this point. The growth of a nucleus is determined by the rate at which an atom can move and attach to the nucleus. Therefore, the growth rate is a diffusion controlled process.

According to Fick's first law, there are two factors that affect the diffusion motion of an atom to a nucleus. First, the driving force is equivalent to the free energy change. Second, the diffusion coefficient of the atoms is proportional to $\exp(-\Delta E/KT)$. Thus, the growth rate could be controlled by controlling the driving force and the diffusion coefficient.

THEORY BEHIND THE MAGNETIC FIELD CONCERNING WATER TREATMENT

Background

Improvement of water treatment has become one of the major problems in industry and electric power production. Water is never naturally pure, as it contains dissolved and suspended solids. These dissolved solids are measured in terms of hardness which, in turn, may be classified into temporary and permanent hardness [12].

Temporary hardness is due to dissolved bicarbonates in water. These bicarbonates can be easily removed by a heating process. Permanent hardness is due to the presence of the sulfates and chlorides of calcium and magnesium, which cannot be removed by heating.

Treatment Methods

For the last century, American industries have used conventional methods to treat water against hardness. Those methods are the chemical treatment of water [12]. Some of these methods are summarized as follows:

a. The ion-exchange process
b. Filtration of water entering a heat exchanger.
c. Addition of hardness stabilizers.
d. Addition of solubilizing chelates.
e. Pump acid through a system to dissolve scales.

These conventional methods have contributed to the problem of water pollution. To overcome this dilemma, scientists and engineers all over the world have searched for a new technology to replace the chemical treatment of water. One new technology is the treatment of water by a magnetic field.

Magnetic Field History

Numerous experiments have been made to reduce or eliminate the existing hardness in water. Two scientists, Welder and Partrige, have run experiments using electric, magnetic field to eliminate the hardness of water [13]. In addition, several articles and papers have been written about the magnetic treatment of water, and have been published in the Soviet Union over the last two decades. Since then, the question still arises as to how a magnetic field acts on water. Investigators in the "magnetic treatment of water" field have shared different theoretical philosophies about this subject, however, their theories are still not well formulated.

Theories of Performance

During the testing period of magnetic treatment of water, conducted by the University of Central Florida, three vendor's products were used in the conduction of the testing performed at the Bayboro power plant. Their theories will be briefly stated in the accompanying paragraphs, followed by a new theory which is being presented in this thesis.

Turbomag

The Turbomag device, Figure 18, consists of an electromagnet surrounding a carbon steel pipe. Although the magnetic field is believed to be of the direct current type, it does not reduce the amount of particles in water. In fact, it only modifies them in such a way that they will not adhere to any surface within the system. This theory is based on the molecular and sub-atomic structure of the particles within the water and water molecules itself. This is accomplished by understanding the Brownian movement, molecular theory, electrophoresis and quantum mechanics [16].

Linear Kinetic Cell

The Linear Kinetic Cell, Figure 19, consisting of an insulated DC magnetic coil, uses a direct current electromagnet which surrounds a section of pipe to effect the water treatment.

The Linear Kinetic Cell (LKC) corporation does not propose its own theory. However, their ideas as to how the LKC system works is stated as follows:

> "Basically, the treatment cell in the LKC system exerts a DC magnetic flux field containing the energy required to orient the molecules or ions of scale-forming minerals which exist in a dipole

FIGURE 18A. TURBOMAG UNIT

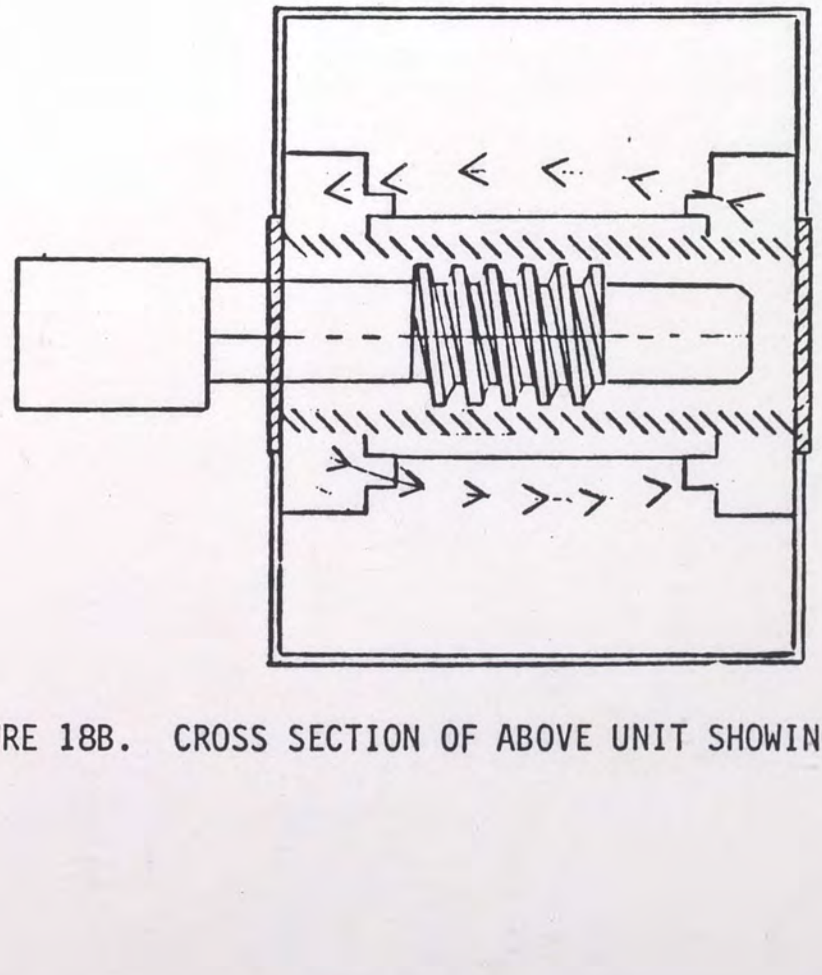

FIGURE 18B. CROSS SECTION OF ABOVE UNIT SHOWING THE FLUX LINES

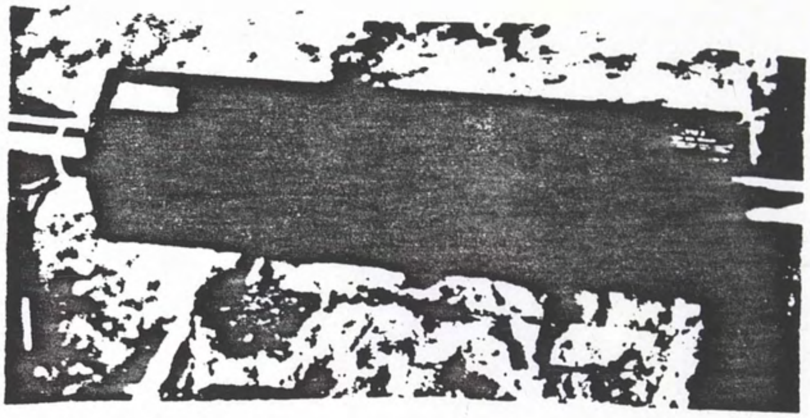

FIGURE 19A. LINEAR KINETIC CELL

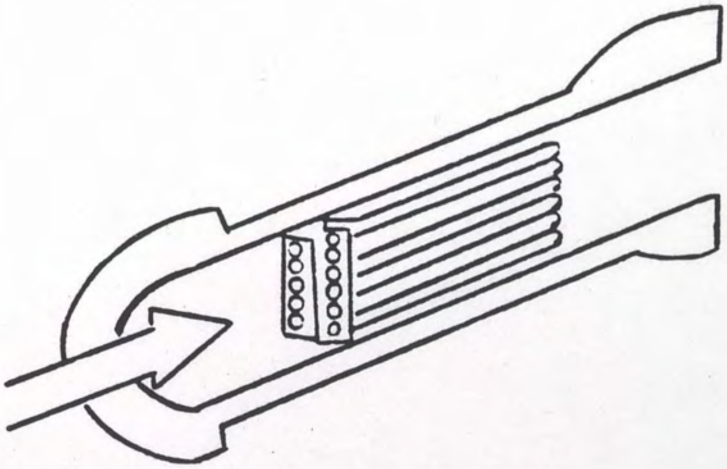

FIGURE 19B. CROSS-SECTION OF THE ABOVE UNIT SHOWING HOW MAGNETIC ARRAYS ARE MOUNTED

> condition in the fluid stream...as a result, a molecular chain is formed by connecting positive and negative charges resulting in a neutral overall charge."[14]

Hydrodynamics

The Hydrodynamic unit, Figure 20, consists of a permanent magnet through which the water is accelerated by a venturi device perpendicular to the magnetic field. The theory includes magneto-hydrodynamics (MHD), magnetisms, and the zeta potential of solids [17].

Introduction to Theory of Operation

At this time, the theories and the philosophical thoughts previously stated will neither be rejected or accepted as accurate. Theory of operation will be based on the actual observation of deposits formed in the condenser's tubes. This theory will be explained from the view point of homogeneous nucleation.

Upon observation, it was discovered that there was uniform distributionof deposits along the inner surface of each tube. Also the chemical composition and the thickness of crystals were the same. In addition, all tubes had received the same quantity and quality of cooling water. Keeping in mind all the above, homogeneous nucleation is a process involving spherical nuclei of β particles which are formed in the α phase. This is considered the

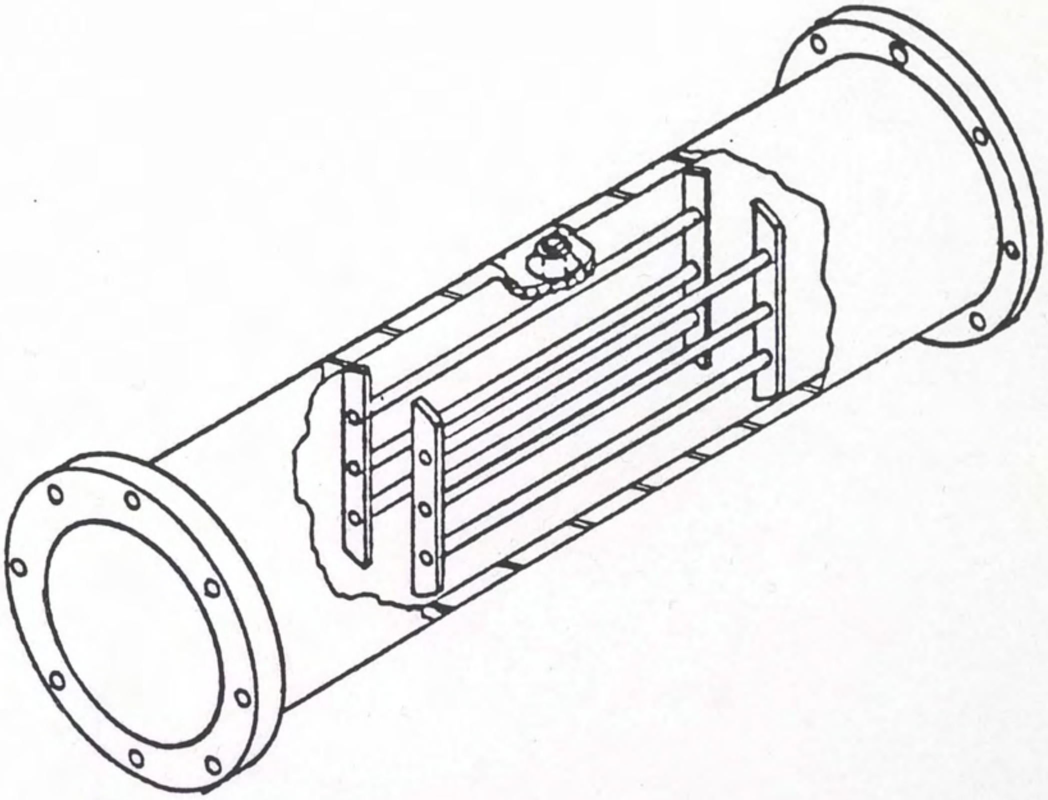

FIGURE 20. HYDRODYNAMICS WATER TREATMENT DEVICE.

ideal process of homogeneous nucleation. Actually, nucleation will occur heterogeneously rather than homogeneously, wherein different sizes and shapes of particles are formed in the phase.

Basically, these processes have the same fundamental equations, and they describe how solidification occurs from the liquid phase to solid. For instance, the coefficients of the terms in Equation 1-29 are based on the assumption that β particles are spherical. But if the particles are not spherical, these coefficients will be different. In this case, the assumption of heterogenous nucleation is impractical and difficult to work with. Once the assumption of homogeneous nucleation is established, the arising question is how the magnetic energy will affect, or improve, the homogeneous nucleation process.

Results and Discussion

When a flow of seawater passes through a magnetic system, the coexisting suspended particles in the water are subjected to physical changes. As these particles pass through the heat exchanger, they are transformed into deposits. The physical changes incurred during this transformation are described as an increase or decrease in the size and the number of particles. The question of how magnetic energy affects the size, number, rate, and growth of particles is addressed in this paper. Before answering this question, other substantial information, and results of tests concerning the chemical analysis and the measurement of deposits thickness will be presented and analyzed. These are necessary to help support the answer to the question posed above.

First, additional substantial information about homogeneous nucleation will be given. According to the reference [18] the following information was stated, "It is often observed that when a substance changes its phase, the phase change begins at a particular location. Therefore, solidification begins at particular locations called nucleation sites. These sites are small solid particles, and they grow according to the solidification models. The formation of homogeneous nucleation sites can be explained in terms of the energy distribution among the liquid atoms. As the temperature of the melt decreases, the number of slow-moving liquid atoms increases. The slow-moving atoms can bond to each other, forming a small solid. This small solid can be considered as spherical in shape." The importance in the above statement is that solidification will occur by the slow movement of atoms. The aggregation of these atoms are considered as spherical in shape. As explained in Chapter 3, if the radius of the described sphere is less than the critical radius, the sphere will revert to the liquid phase, which is called embryo. If the radius of the sphere is larger than the critical radius, it is called a nucleus. This nucleus serves as the creation source of a crystal.

Another important point in the above statement also must be considered. This is the temperature factor. Obviously, the temperature factor is one among other major parameters that control nucleation. To demonstrate the importance of this factor, an example will be given and analyzed. Since no data, at the atomic level, was available for the deposits found in the condenser's tubes, this example will consider silver as the deposits. Silver is chosen because of the availability of the data at the atomic level [1]. The numerical values given in this example might be applied to deposits found in the condenser's tubes. Once again, this example is given for clarity and demonstration.

The solid-liquid interfacial energy of silver, γ, is 126 ergs/cm^2. The latent heat is 25 cal/g, the melting temperature is 961C. The density of solid or liquid silver is 10.5 g/cm^3. It is desired to find the value of r^* at 700C [19].

The answer to this problem is fairly easy. First, it can be noticed that solidification will occur homogeneously. Therefore, heat is envolved and the latent heat (ΔE_V) is negative. Hence, applying Equation 1-32, the value of r^* is equal to 22 Angstron.

The above example shows that the value of the critical radius was calculatd at a specific temperature. If these given temperatures were different, the value of the critical radius would be different. Now what if solidification occurs at a low temperature (80F). In this case, the temperature factor would be insignificant and could be considered as a constant. These conditions are found in the cooling seawater used to cool the condenser's tubes. The supply inlet water temperature was found to be equal to 80F, whereas ΔT across the condenser was equal to 0.5F.

In spite of the existence of these low temperatures, deposits were formed around the inner surface of the tubes.

Secondly, other useful information based on graphical interpretation will be presented. According to reference [20]:

> "When the nucleation rate is low but the growth rate is high, only a relatively few nuclei will form. Therefore, the grains will be large. Alternatively, when the nucleation rate is high and the growth rate is low, many nuclei will form. Hence, the average size of phase grains (crystals) will be small."

These thoughts can be applied to deposits that were formed in the heat exchanger tubes during the Florida Power test. Deposits are referred to as crystals, which accumulate on top of one another. These crystals are composed of molecules, which in turn are composed of atoms. A small aggregation of atoms will form a solid. This solid is called a nucleus, where one crystal is capable of growing from each nucleus. As deposition progresses, the crystals will join each other and form boundaries, as shown in Figure 21. Deposits are composed from boundaries connected to each other by interatomic forces. The dimensions of these boundaries will depend on the size of crystals. If the size of crystals is large, the boundaries are going to be large. Therefore, this will result in the production of crusty and hard deposits. In contrast, if the size of crystals is small, the boundaries are going to be small. Hence, this will yield

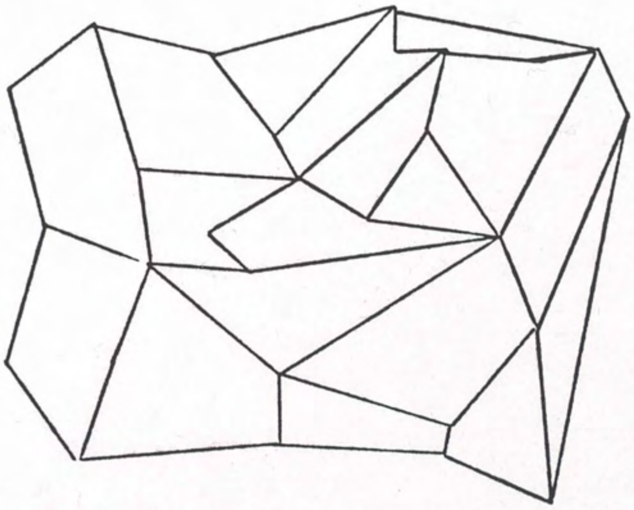

FIGURE 21. SCHEMATIC DIAGRAM OF CRYSTALS GROWING TOGETHER FORMING GRAIN BOUNDARIES.

soft powder-like deposits. Thirdly, the results obtained from the actual test will be presnted. It was observed that deposits found in tubes, which received treated seawater from the Turbomag unit, Linear Kinetic cell unit, or Hydrodynamic unit, were suspended freely along the inner surface of the tubes. In addition, these deposits were flaky (powder-like), and showed a high degree of dryness. In contrast, deposits found in tubes, which received untreated seawater, were fairly adhered to the inner wall of these tubes. Furthermore, these deposits were crusty and showed a low degree of dryness.

In spite of these physical differences between the deposits, the chemical analysis and the thickness of the deposits in all tubes showed no significant difference. As a matter of fact, the chemical analysis was the same.

So far, nothing has been proved, mathematically, as to how the magnetic energy effects the size, number, rate and growth of particles. Consider the example noted above as a model to estimate numerically the size, the number, the rate, and the growth of particles with and without the magnetic energy. Then the results of this task will be related to deposits found in the condenser's tubes.

Before starting the process of estimation, it is necessary to make some changes in the given of the example, so these changes can meet the requirement of the actual problem. These requirements are the formation of crystals under very low temperature (80F).

Therefore, the temperature is going to be considered as a constant throughout the whole analysis. In addition, it would be practical to assume some numerical value for the critical radius of the sphere. This value will correspond to the sphere that might formed in deposits found in tubes that received untreated water. The value of r^* found in the above example will be used as a reference value. Therefore, r^* is equal to 22A taking in consideration that the temperature is a constant. Keeping in mind all the list assumptions, it is very important to remember that homogeneous nucleation is the process responsible or the formation of crystals in all the condenser's tubes.

With the assumptions made above, the modified question will be posed in the following manner: "What is the value of r^* at low temperatures and in the presence of a magnetic field?" The solution will start by considering Equation 1-14, which is the mathematical form of the first and second law of thermodynamics. This equation will be modified if magnetic energy is added to it. Thus the result will be:

$$\Delta G_m = \Delta E - T\Delta S - \Delta M \qquad (1\text{-}35)$$

where ΔG_m is the free energy change in the presence of magnetic energy, and M is the change in magnetic energy.

According to the kinetic phase changes that were discussed in the previous chapter, Equation 1-35 can be rewritten on the basis of bulk or volume free energy. The result will then be:

$$\Delta G_{vm} = \Delta E_v - T\Delta S_v - \Delta M_v \qquad (1\text{-}36)$$

At equilibrium (see discussion for the kinetic phase changes in the previous chapter) $\Delta G_{vm} = 0$, and Equation 1-36 will reduce to the following:

$$\Delta E_v - T\Delta S_v - \Delta M_v = 0$$

$$\Delta S_v = (\Delta E_v - \Delta M_v)/T_e \qquad (1\text{-}37)$$

Substitute Equation 1-37 into 1-36 and rearrange.

$$\Delta G_{vm} = \Delta E_v - T\ \left(\frac{\Delta E_v - \Delta M_v}{T_e}\right) - \Delta M$$

or

$$\Delta G_{vm} = \Delta E_v - T/T_e(\Delta E_v) + T/T_e(\Delta M_v) - \Delta M_v$$

rearrange the above equation

$$\Delta G_{vm} = \Delta E_v - \frac{T}{T_e}\ (\Delta E_v) + \frac{T}{T_e}\ (\Delta M_v) - \Delta M_v$$

$$\Delta G_{vm} = \Delta E_v\ \left(\frac{T_e - T}{T_e}\right) + \Delta M_v\ \left(\frac{T - T_e}{T_e}\right)$$

The following form of the above equation could be reduced to the following:

$$\Delta G_{vm} = \Delta E_v(\Delta T/T_e) - (\Delta T/T_e)\Delta M_v \qquad (1\text{-}38)$$

where $\Delta T = T_e - T$ and $T - T_e = -\Delta T$.

Since ΔT is very small, and T_e is constant, the term $\Delta T/T_e$ will be replaced by using the constant K_1. Thus Equation 1-38 will be written in the following manner:

$$K_1(\Delta E_v) - K_1(\Delta M_v) = K_1\ (\Delta E_v - \Delta M_v) \qquad (1\text{-}39)$$

Once Equation 1-39 is established, it will be substituted into Equatin 1-32, and the result of this substitution will be as follows:

$$r^*_2 = \frac{-\ 2\gamma}{K_1\ (\Delta E_V - \Delta M_V)} \qquad (1\text{-}40)$$

where r^*_m is the critical radius of nuclei in the presence of magnetic energy.

Substituting Equation 1-39 into 1-33, the result will be as follows:

$$\Delta G^*_m = \frac{16\ \pi\ \gamma^3}{3K_1^2\ (\Delta E_v - \Delta M_v)^2} \qquad (1\text{-}41)$$

where ΔG^*_m is the critical free energy in the presence of magnetic energy.

The above derivation shows that r^*_m is less than r^* (untreated water). This is due to the fact that the magnetic energy change factor is in the denominator. Therefore, the estimated value of r^*_m would decrease. Hence, these results show that the size of treated nuclei that have sufficient thermal energy to form, will be smaller than the size of the untreated (were not exposed to magnetic energy) nuclei. As a result, it is concluded that the size of treated crystals, which will grow from each nuclei, will be smaller than the untreated crystals.

Similarly, from the above derivation, it can be seen that ΔG^*_m is much less than ΔG^*. This improvement in decreasing the barrier height of the critical free energy, by the magnetic energy, will allow the nuclei β to be in a much more stable state. In other words, the number of treated nuclei is increaed tremendously. The results concerning r^*_m and ΔG_{*m} can be interpreted graphically, as in Figure 22. A similar figure was provided in Chapter 3. Comparison between the two graphs that represent total free energy and bulk free energy reveals that the magnetic energy is expected to shift, downward and to the left. In addition, it is expected to be a slight change in the graph that represents the surface energy term. However, this slight change could be neglected because of the unknown effects of the magnetic energy on the surface energy term to this date.

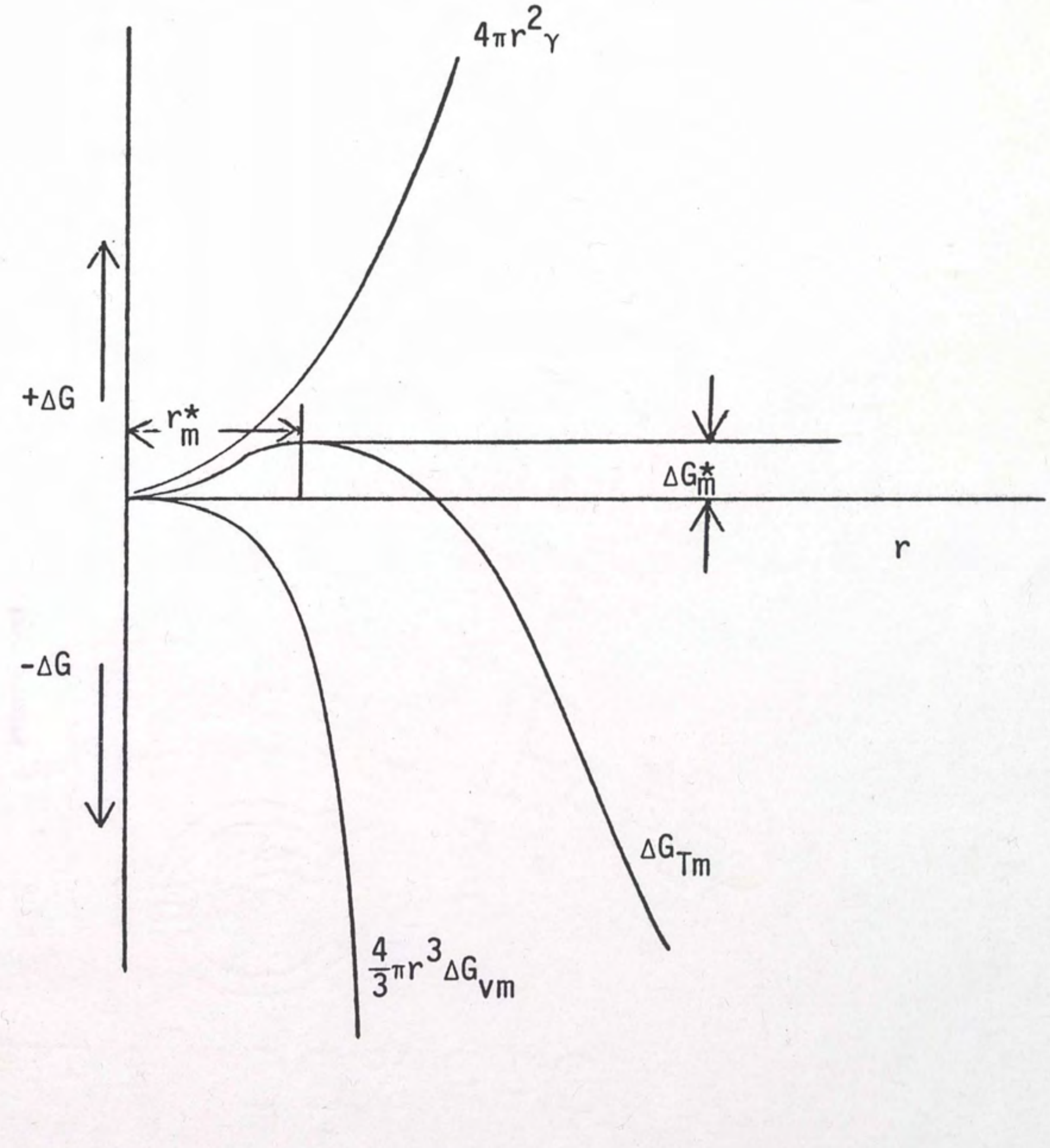

FIGURE 22: NUCLEATION OF MAGNETICALLY SPHERICAL SOLID NUCLEI

Briefly, the magnetic energy reduces the size of nuclei, and increases their numbers. Based upon these results, it can be deduced, automatically, that the magnetic energy increases the rate of nucleation and decreases the growth rate of nuclei. Hence, the results of actual observations of the treated deposits agree with the proposed theory presented in this paper.

CONCLUSIONS

A study concerning the effects of magnetic field on seawater has been completed. The main objective behind this study was to evaluate the effectiveness of magnetic field on saltwater. Based upon the actual observations, a decision may be made to replace the old methods of tube cleaning by the new methods. The old methods involve the use of chemical agents in order to clean, or reduce the amount of deposition on condenser's tubes. The new method involves the use of magnetic devices that supposedly function as chemical agents. Scattered throughout the text material are the results, and the conclusions of this study. It is beneficial to summarize these thoughts in the following few pages.

Three different types of magnetic tubes were tested. These were the Turbomagnetic unit, Linear Kinetic Cell, and the Hydrodynamic unit. The magnetic flux in each unit was oriented differently, but all three showed similar effects on the deposits. Therefore, it can be concluded that the method of producing the magnetic field is not of primary importance. Measurement of deposits thicknesses in tubes that received treated and untreated seawater were insignificant. However, it was discovered that the magnetic field was more effective in warmer saltwater. In other words, the reduction in the average amount of deposits in summer time was higher than in winter time. The chemical analysis indicated that all the deposits contained the same compounds and elements. In spite of these common characteristics, the deposits on the tubes from the treated section were more easily removed and less adherent to the wall of the tubes. In contrast, the deposits on the tubes from the untreated section were more adherent, and harder to remove. Finally, the heat transfer analysis indicated that the built-up deposits in both sections, treated and untreated, would approach similar reduction in heat transfer.

Theoretically, it was demonstrated that the magnetic energy did decrease the size of nuclei, and increase their numbers. Therefore, the rate of nucleation is increased, and the growth rate of nuclei is decreased. These results were in agreement with the actual observations.

In summary, the use of any magnetic device as a chemical agent to condition seawater does not appear to be effective or useful.

RECOMMENDATIONS

This study was conducted to test the concept of using magnetic devices as a substitute for chemical agents in seawater. The results obtained from the test program did not support the use of these devices in power plant's condensers. However, it was observed that the magnetic energy did slightly condition the seawater that was being used as cooling water in the condenser. The conditioning process was explained from the view point of the homogeneous nucleation process. Therefore, future investigation should include detailed research in this area, at the atomic level. In the next paragraphs, some suggestions will be given which might lead to a solution of the problem.

The first suggested solution is to look for a new system that would increase the barrier height of the critical free energy so that a stable nucleus cannot form and grow. This new technique may eliminate the existence and the formation of deposits.

It was experienced by an investigator that the treated five-inch piece of tubing had deposits that were more easily removed by tapping this piece on a solid surface. In other words, an external small force was needed in order to shake off all the deposits. If the magnitude of this force is measured or calculated, its value can be used as a guide to see how much extra energy the magnetic device needs to prevent the adherence of deposits on tube's wall.

Finally, it was concluded in Chapter 2, that the magnetic field was more effective in the summer time. Therefore, future investigations should be forcused on how the magnetic field will effect the suspended particles in warm and cold seawater. The investigation could be an experiment in a laboratory using a small model of the described test program in Chapter 2. In the laboratory it would be very easy to control the inlet cooling water. Once the water temperature is under control, the study should be narrowed to the behavior of the activation energy that might be affected by the magnetic energy.

END NOTES

[1] M. M. Eisenstadt, Introduction to Mechanical Properties of Materials, (New York: MacMillan Publishing Co., Inc., 1971): pp. 23-27.

[2] Ibid., p. 35.

[3] C. R. Barrett, W. D. Nix and A. S. Tetelman, The Principles of Engineering Materials, (Englewood Cliffs, New Jersey: Prentice-Hall, 1973): p. 24.

[4] M. M. Eisenstadt, Introduction to Mechanical Properties of Materials, (New York: MacMillan Publishing Co., Inc., 1971): pp. 114-116.

[5] C. R. Barrett, W. D. Nix and A. S. Tetelman, The Principles of Engineering Materials, (Englewood Cliffs, New Jersey: Prentice-Hall, 1973): pp. 145-150.

[6] Ibid., pp. 150-156.

[7] M. M. Eisenstadt, Introduction to Mechanical Properties of Materials, (New York: MacMillan Publishing Co., Inc. 1971): pp. 284-286.

[8] C. R. Barrett, W. D. Nix and A. S. Tetelman, The Principles of Engineering Materials, (Englewood Cliffs, New Jersey: Prentice-Hall, 1973): pp. 161-163.

[9] J. H. Brophy, R. M. Rose and J. Wulff, The Structure and Properties of Materials, (New York: John Wiley and Sons, 1964): pp. 99-102.

[10] C. R. Barrett, W. D. Nix and A. S. Tetelman, The Principles of Engineering Materials, (Englewood Cliffs, New Jersey: Prentice-Hall, 1973): p. 166.

[11] Ibid., p. 168.

[12] A. R. Ergun, "Treatment of Water by Force Fields - Biological and Medical Implications," Bogazici Universitesi Dergisi: Muhendislik 2, (May 1974): pp. 3-4.

[13] G. Kvajic and M. Milosevic-Kvajic, "Magnetic Field Conditioning of Industrial Waters," The International Water Conference 40th Annual Meeting 13, (April 1979): p.156.

[14] Magnetics, Inc., "Frequently Asked Questions about the L-K-C Magnetics Systems," (San Diego, CA: Magnetics, Inc. 1982): p. B-7.

[15] E. R. Hosler, R. L. Henry, and M. A. Nehme, "An Investigation of the Effects of Magnetic Flux on the Prevention of Condenser Tube Scale in Seawater," Final Report to Florida Power Corporation, UCF Report NO. ENGR84-85-2, April 1985.

[16] "Theory of Turbomag Electromagnetic Water Treatment," (Miami: Turbomag Corporation, 1982): p. 1.

[17] J. F. Grutsch and J. W. McClintock, "Corrosion and Deposit Control in Alkaline Cooling Water Using Magnetic Water Treatment at Amoco's Largest Refinery," Corrosion 84 1 (April 1984): pp. A60-A62.

[18] M. M. Eisenstadt, Introduction to Mechanical Properties of Materials, (New York: MacMillan Publishing Co., Inc., 1971): p. 99.

[19] C. R. Barrett, W. D. Nix and A. S. Tetelman, The Principles of Engineering Materials, (Englewood Cliffs, New Jersey: Prentice-Hall, 1973): p. 164.

[20] C. R. Barrett, W. D. Nix and A. S. Tetelman, The Principles of Engineering Materials, (Englewood Cliffs, New Jersey: Prentice-Hall, 1973): p. 169.